THE EFFECT OF ITACONIC ACID ON MITOCHONDRIAL SUBSTRATE-LEVEL PHOSPHORYLATION

PhD Thesis

Beáta Németh

János Szentágothai Doctoral School of Neurosciences

Semmelweis University

Supervisor:	Christos Chinopoulos, MD, Ph.D
Official Reviewers:	Zsuzsa Szondy, MD, D.Sc
	Tamás Kardon, MD, Ph.D
Head of the Final Examination Committee:	József Mandl, MD, D.Sc
Members of the Final Examination Committee:	Balázs Sarkadi, MD, D.Sc
	Károly Liliom, Ph.D

Budapest
2017

"Discovery consists of seeing what everybody has seen,
and thinking what nobody has thought."
Albert Szent-Györgyi

TABLE OF CONTENTS

1. THE LIST OF ABBREVIATIONS

Acod1	*cis*-aconitate decarboxylase 1 gene (previous name: immunoresponsive gene 1, *Irg1*) (in mouse)
Acod1	*cis*-aconitate decarboxylase 1 protein (previous name: immunoresponsive protein 1, Irg1) (in mouse)
ADP	adenosine 5'-diphosphate
ANT	adenine nucleotide translocase
ATP	adenosine 5'-triphosphate
BKA	bongkrekic acid (ANT inhibitor)
BMDM	bone marrow-derived macrophages
CAD	*cis*-aconitate decarboxylase protein (in fungus *Aspergillus terreus*)
cad1	*cis*-aconitate decarboxylase gene (in fungus *Aspergillus terreus*)
cATR	carboxyatractyloside (ANT inhibitor)
DNP	2,4-dinitrophenol (uncoupler)
ECAR	extracellular acidification rate
ETC	electron transport chain
FAD	flavin adenine dinucleotide (oxidized form)
$FADH_2$	flavin adenine dinucleotide (reduced form)
FMN	flavin mononucleotide (oxidized form)
GABA	γ-aminobutyric acid
GDH	glutamate dehydrogenase
GDP	guanosine 5'-diphosphate
GTP	guanosine 5'-triphosphate
KGDHC	α-ketoglutarate dehydrogenase complex
LPS	lipopolysaccharide
MGTK	methylglutaconase (methylglutaconyl-CoA hydratase)
$NAD(P)^+$	nicotinamide adenine dinucleotide (phosphate) (oxidized form)
NAD(P)H	nicotinamide adenine dinucleotide (phosphate) (reduced form)
OCR	oxygen consumption rate
P_i	inorganic phosphate
ROS	reactive oxygen species
SDH	succinate dehydrogenase

SF 6847	3,5-di-tert-butyl-4-hydroxybenzylidenemalononitrile (uncoupler)
siRNA	short-interfering RNA
SLP	substrate-level phosphorylation
STK / SUCL	succinate thiokinase / succinate-CoA ligase (succinyl-CoA synthetase)
TAMs	tumor associated macrophages
TCA	tricarboxylic acid cycle (citric acid cycle)
TIPM	thioglycollate-induced peritoneal macrophages
TLR	Toll-like receptor
TMRM	tetramethylrhodamine methyl ester
$\Delta\Psi m$	mitochondrial membrane potential

2. INTRODUCTION

Itaconic acid, matrix substrate-level phosphorylation (SLP) and macrophages represent the main focus of this thesis. From a more general point of view, it is about immune cell specific metabolism.

Usually, metabolism is viewed as the function of cells generating a store of energy by catabolism, and to synthesizing macromolecules for cell maintenance and growth through anabolic pathways. However, today we know that there are some disorders, such as diabetes, atherosclerosis, cancer, inflammatory conditions, in which there are obvious dysfunctions in metabolism. In early 1900s Otto Warburg proposed that metabolic dysregulation was a feature of tumor cells (Warburg, 1923). The German biochemist discovered that when oxygen becomes limiting, mitochondrial oxidative metabolism is restricted in tumor cells, *i.e.*, the cancer cells take up large amounts of glucose and metabolize it to lactic acid, even in the presence of oxygen. This process has become known as the Warburg effect.

There is an emerging field of interest in studies of immune system metabolism (immunometabolism). The aim of these investigations are: how immune cells function in terms of their intracellular metabolism, how these metabolic pathways affect the phenotype and activation of immune cells, and how the immune system affects the metabolic functions of its host organism (Pearce et al., 2013).

Studies on murine macrophages uncovered a gene, *cis*-aconitate decarboxylase 1 (*Acod1*), as one of the most highly expressed gene under pro-inflammatory conditions, which product, *cis*-aconitate decarboxylase 1 protein (Acod1), is associated with mitochondria (Degrandi et al., 2009). Furthermore, experiments revealed that in mammalian cells Acod1, similarly to *cis*-aconitate decarboxylase (CAD) in fungus *Aspergillus terreus*, synthesizes itaconic acid through decarboxylation of the tricarboxylic acid (TCA) cycle intermediate *cis*-aconitic acid (Michelucci et al., 2013). The same metabolite, itaconic acid, was discovered in lipopolysaccharide (LPS)-activated macrophages (Strelko et al., 2011).

In the mitochondrial matrix, as the part of TCA cycle, succinate-CoA ligase (SUCL) catalyzes the reversible conversion of succinyl-CoA and ADP (or GDP) to CoASH, succinate and ATP (or GTP) (Figure 1). This reaction is known as substrate-level phosphorylation, and plays a critical role in producing high-energy phosphates in

mitochondria − it is the only means of ATP (or GTP) source under hypoxia or impaired electron transport chain (ETC). In murine macrophages itaconic acid and SLP are placed within the same compartment, that is, in the mitochondria. Whatsoever, itaconate is formed from the TCA cycle intermediate, and at the same time, SLP is also part of TCA cycle. The consideration arises: Does itaconic acid have any impact on SLP, or not?

In isolated mitochondria, the TCA cycle, that is, the operation or not of SLP could be manipulated using different substrates (for details see: "Categorization of respiratory substrates used for isolated mitochondria"). The functionality of SLP is essential during compromised ETC. Under experimental conditions different inhibitors of the complexes of the ETC are used to mimic respiratory chain failure. Changes in operation of SLP are deduced from directionality of adenine nucleotide translocase (ANT). In the experiments using "biosensor test" (Figure 3) the effect of ANT inhibitor on mitochondrial membrane potential ($\Delta\Psi m$) during ADP-induced respiration is examined. $\Delta\Psi m$ is estimated using fluorescence quenching of a cationic dye, which accumulates inside energized mitochondria. As the hypothesis through this thesis is that itaconate affects SLP, any of its effects could be detected using "biosensor test".

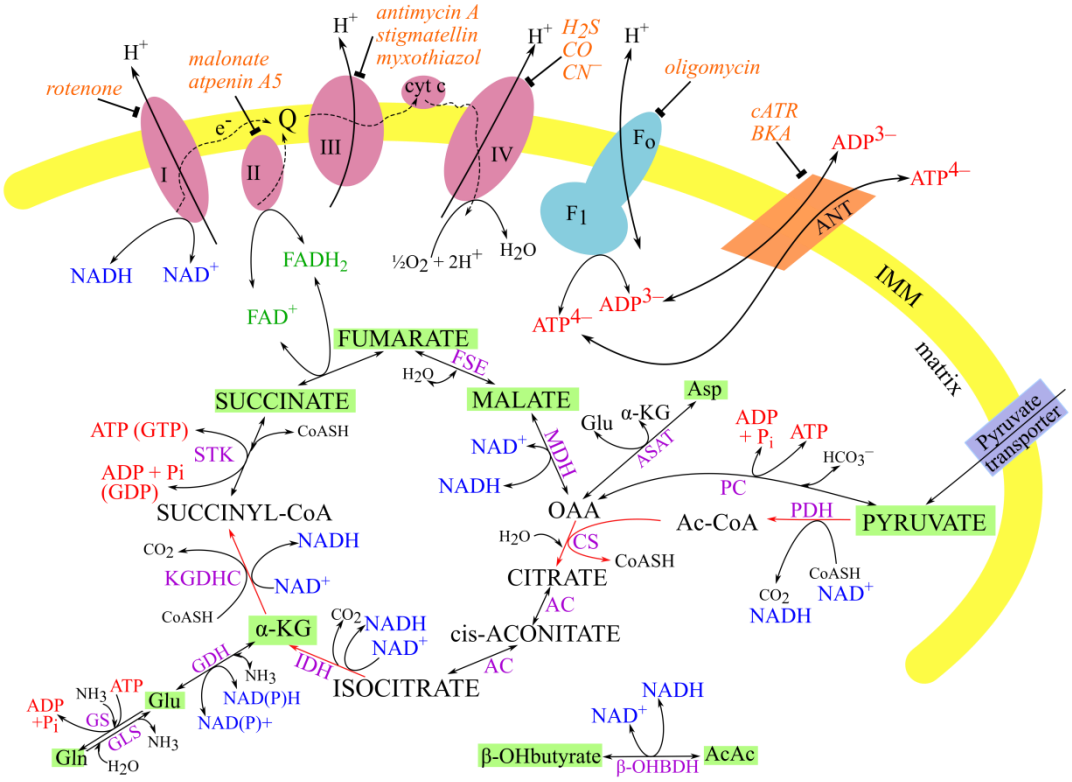

Figure 1. Schematic representation of TCA cycle and ETC. *Electron carriers, NADH and $FADH_2$, transduce their reducing equivalents to the ETC (shapes in magenta) through C-I and II. CoQ serves as a mobile carrier of electrons as well as cytochrome c. Electron flow through C-I, III and IV is accompanied by proton flow from the matrix to the intermembrane space. The overall proton gradient across the inner mitochondrial membrane (IMM) drives the phosphorylation of ADP to ATP by F_o-F_1 ATP synthase. The complex-specific inhibitors are shown in orange. ANT, adenine nucleotide translocase; BKA, bongkrekic acid; cATR, carboxyatractyloside; P_i, inorganic phosphate; OAA, oxaloacetate; α-KG, α-ketoglutarate; Gln, glutamine; Glu, glutamate; Asp, aspartate; AcAc, acetoacetate; β-OHBDH, β-hydroxybutyrate dehydrogenase; PDH, pyruvate dehydrogenase; PC, pyruvate carboxylase; CS, citrate synthase; ASAT, aspartate aminotransferase; AC, aconitase; GS, glutamine synthetase; GLS, glutaminase; GDH, glutamate dehydrogenase; IDH, isocitrate dehydrogenase; KGDHC, α-ketoglutarate dehydrogenase complex; STK, succinate thiokinase; FSE, fumarase; MDH, malate dehydrogenase. Substrates used to manipulate SLP in isolated mitochondria are highlighted in green (for details see: "Categorization of respiratory substrates used for isolated mitochondria").*

2.1. Metabolism − the hub of biochemical activities

Metabolism is sometimes overlapping cross-talk of different and complex biochemical pathways. This great hub of interconnected chemical changes incorporates two contrasting processes, catabolism and anabolism. These two mechanisms together constitute the chemical pathways of reactions that convert food into usable forms of energy and structured biomolecules. Catabolism, in other means the degradation of ingested food or stored fuels (carbohydrates, lipids and proteins), generates either usable or storable forms of energy. As a result of catabolic reactions complex biomolecules are converted to smaller ones, such as carbon dioxide (CO_2), water (H_2O), ammonia (NH_3). In mammals, this process usually requires consumption of oxygen. Oxidative breakdown of food is linked to energy-production and releasing of reducing power. The energy released during catabolic processes is used to ATP synthesis, furthermore reduced electron carriers are also obtained (NAD(P)H and $FADH_2$), and some of the energy is lost as heat. On the other hand, anabolic pathways are in charge of biosynthesis of large molecules from smaller precursors by energy utilization processes – it requires the phosphoryl group transfer potential of ATP and the reducing power of NAD(P)H and $FADH_2$. Biochemical reactions based on energy mobilization perform various important functions − for example, nerve impulse conduction, muscle contraction, active ion transport, thermogenesis, cell growth and division.

ATP, an interchangeable currency in living organisms, is the essential link between energy-producing and energy-utilizing pathways. Hydrolysis or more precisely the transfer of phoshoryl, pyrophosphoryl, or adenylyl group from ATP to substrates results in coupling the energy of ATP breakdown to energy-utilizing reactions. Under physiological conditions ATP is chelated with a divalent magnesium cation (Jahngen and Rossomando, 1983).

2.2. Immune system − patrolling, guarding and eliminating keeper of the gates

The immune system is the body's own defense system against pathogens. This sensitive and specific biochemical system is capable of distinguishing molecular "self" from "non-self". In this way the immune system eliminates those entities that may pose a threat to the organism. The immune response to an invader is an intricate and coordinated set of interactions among many classes of proteins, molecules and cell types

(Nelson and Cox, 2008). A specialized array of cells arises from undifferentiated stem cells in the bone marrow − a variety of leukocytes, including macrophages and lymphocytes.

From our point of view macrophages are of the interest in this work, and let it be given a somewhat detailed overview of them.

2.3. Macrophages − the big eaters

Macrophages were originally identified by Ilya Metchnikoff more than 100 years ago (Nathan, 2008). These large, amoeba-like cells are terminally differentiated cells of the immune system. They do not need energy and biomass to proliferate but instead to sustain a high phagocytic and secretory activity. Macrophages, found in all tissues, play crucial roles in innate immunity and can respond to local immune- and/or pathogen-derived signals to adopt different activation states (Mantovani et al., 2013).

Macrophages are by origin leukocytes and may have different names according to where they function in the body. They are termed: alveolar macrophages – in lung; Kupffer cells – in liver; microglia – in central nervous system; splenic macrophages – in spleen marginal zone, red and white pulp.

Macrophages recognize the pathogens *via* Toll-like receptors (TLRs). These evolutionarily conserved receptors are a group of special receptors called PRRs (Pattern-Recognition Receptors) which recognize conserved microbial structures called PAMPs (Pathogen-Associated Molecular Patterns) or DAMPs (Danger-Associated Molecular Patterns) that are endogenous molecules released from necrotic or dying cells. TLRs are homologues of the *Drosophila* Toll protein, discovered to be important for defense against microbial infection. PAMPs, exclusively expressed by microbial pathogens, include various bacterial cell wall components such as LPS, peptidoglycan and lipopeptides, as well as flagellin, bacterial DNA and viral double-stranded RNA. DAMPs include intracellular proteins such as heat shock proteins as well as protein fragments from the extracellular matrix (Rosin and Okusa, 2011).

The major structural component of the outer wall of all Gram-negative bacteria, LPS, is recognized by Toll-like receptor 4 (TLR4). Ten human and twelve murine TLRs have been characterized, TLR1 to TLR10 in humans, and TLR1 to TLR9, TLR11,

TLR12 and TLR13 in mice, the homolog of TLR10 being a pseudogene. TLRs are characterized by an extracellular domain containing leucine-rich repeats and a cytoplasmic tail that contains a conserved region called the Toll/IL-1 receptor domain. LPS consists of a polysaccharide region that is anchored in the outer bacterial membrane by a specific carbohydrate lipid moiety termed lipid A. Lipid A is responsible for the immunostimulatory activity of LPS.

Macrophages undergo specific differentiation depending on the local tissue environment. The concept of classic and alternative activation of macrophages has been in practice since the 1990s when it was discovered that the cytokine interleukin (IL)-4 induced different effects on macrophage gene expression compared to that of interferon (IFN)-γ and LPS. Later, in 2000, Mills and colleagues proposed a new terminology for macrophage classification (Mills et al., 2000). The scientific community accepted that M1 (classically activated) macrophages exhibit inflammatory functions, whereas M2 (alternatively activated) macrophages exhibit anti-inflammatory functions. Today the M1/M2 classification of macrophages is considered an oversimplified approach. For example, the tumor associated macrophages (TAMs) do not fit into the criteria of M1 or M2 macrophages (Qian and Pollard, 2010); furthermore, macrophages expressing T cell receptors (TCR) and CD169 have also been identified (Qi Chávez-Galán et al., 2015).

M1 and M2 activation is characterized by distinct metabolic states, which differ from those of resting macrophages (Rodríguez-Prados et al., 2010). M1 macrophages, activated by LPS and IFN-γ, undergo a switch from oxidative phosphorylation to glycolysis, similar to Warburg effect in tumors. Most of the glucose is converted to lactate, with little being used for oxidative phosphorylation. Even though glycolysis is an inefficient means of ATP production compared to the TCA cycle, still it could be a mechanism to rapidly generate ATP. How does LPS promote switch from oxidative phosphorylation to glycolysis? There are at least four main processes (Kelly and O'Neill, 2015). i) LPS increases the expression of inducible nitric oxide synthase (iNOS), which generates nitric oxide, a reactive nitrogen species that can inhibit oxidative phosphorylation. ii) In LPS-induced macrophages the expression of hypoxia-inducible factor-1α (HIF-1α) is increased, which increases the expression of its target genes, and leads to increased glycolytic flux. iii) LPS causes a marked change from expression of 6-phosphofructo-2-kinase (encoded by PFKFB1) to the PFKFB3 isoform

thereby increasing levels of the metabolite fructose-2,6-bisphosphate. The later one activates the glycolytic enzyme 6-phosphofructo-1-kinase. iv) LPS inhibits AMP-activated protein kinase, resulting in decreased β-oxidation of fatty acids and mitochondrial biogenesis. Further feature of classically activated macrophages is the increased flux through the pentose phosphate pathway, which provides purines and pyrimidines for biosynthesis in the activated cell. M1 macrophages are known to release reactive oxygen species (ROS) and reactive nitrogen species (including NO) in phagosomes serving as a mechanism of pathogen killing (West et al., 2011). To phagocyte, a large turnover of membrane is required; therefore, macrophages increase phospholipid synthesis and switch from cholesterol to phosphatidylcholine production (Ecker et al., 2010). In contrary, M2 macrophages, activated by IL-4, have low glycolysis rates, but perform high fatty acid oxidation and oxidative phoshporylation rates (Vats et al., 2006).

Macrophages are known to be associated with solid tumors (Gordon and Taylor, 2005). They can be recruited to the tumor site from surrounding tissues (Kitamura et al., 2015). Studies have shown that TAMs can express both M1 and M2 polarization fenotypes (Allavena et al., 2008). Notably, switching TAMs to a predominantly M1 phenotype has been proposed as a key anti-cancer immunotherapeutic treatment strategy (Mills et al., 2016). TAMs are known to promote tumor progression (Komohara et al., 2014). They induce angiogenesis, lymphogenesis, stroma remodeling and immune suppression. They also play a key role in promoting tumor invasion and metastasis (Komohara et al., 2016).

Efforts to fully understand macrophage functions involve *in vitro* studies of primary macrophage populations or macrophage-like cell lines. They are suitable for the study of cellular responses to microbes and their products. Through this thesis the following macrophage lines are mentioned: RAW-264.7 cells, BMDM cells, TIPMs.

RAW-264.7 cells are macrophage-like, Abelson leukemia virus transformed cell line derived from BALB/c mice. This cell line is a commonly used model of mouse macrophages for the study of cellular responses to microbes and their products.

Bone marrow-derived macrophages (BMDM), as it stands in the name, they are derived from bone marrow cells. They are primary cells, cultured *in vitro* in the presence of growth factors. Compared to other primary cells, the BMDM are

homogenous, have a proliferative capacity, are transfectable, and have a lifespan longer than a week.

Thioglycollate-induced peritoneal macrophages (TIPMs) are used as primary macrophages in lots of studies, mainly because they are easy to obtain. The peritoneal cavity harbors a number of immune cells including macrophages, B cells and T cells, and is a preferred site for the collection of *naïve* tissue resident macrophages.

2.4. Substrate-level phosphorylation in the mitochondria

Mitochondria are double-membrane-bound compartments, which range in size between 1 and 10 μm in length. They occur in numbers that directly correlate with the cell's level of metabolic activity. The morphologies of these subcellular organelles vary among different cell types. As an example, fibroblast mitochondria are usually long filaments, whereas hepatocyte mitochondria are more uniformly spheres or ovoids. When mitochondria are observed in live cells in electron micrographs, it is apparent that they are far more dynamic than static organelles. Combined action of fission and fusion continually changes their shapes, resulting in extended reticular networks of mitochondria (Youle and van der Bliek, 2012).

As mitochondria move within cytoplasm, they often appear to be the favored "cargoes" of microtubules (Yaffe, 1999). This association with microtubules may determine the unique orientation and distribution of mitochondria in different types of cells − for example, it can form long moving chains (packed between adjacent myofibrils in a cardiac muscle), or remain fixed in one position (wrapped tightly around the flagellum in a sperm).

Mitochondria play a key role in ATP synthesis, and are important in other cellular processes, including fatty acid synthesis, Ca^{2+} homeostasis, ROS production and the biogenesis of hem and iron-sulfur proteins.

Mitochondria, sometimes termed the "powerhouse" of the cell, can decide upon "whether to live, or die" by releasing adequate signals to the environment. "To live" means synthesizing ATP and suppling it to the body's energy requiring processes; "let die" means suspension of ATP synthesis and facilitating signal cascade transduction utilizing apoptotic and necrotic reactions. Cytochrome c, known to be an electron carrier

within the inner mitochondrial membrane, is among activators of caspases, the central executioners during apoptosis. This little but powerful organelle is like a two edged sword. One compartment that is enclosing two opposing features – it is the powerhouse of the cell and its arsenal, too.

Most of the energy in animal cells is produced during oxidative phosphorylation in the mitochondria. This process occurs through passing electrons along a series of carrier molecules, called the electron transport chain. As earlier mentioned (see: "Metabolism – the hub of biochemical activities"), electron carriers, such as NAD(P)H and $FADH_2$, transduce their reducing equivalents to the enzymes of the electron transport chain. The electron transport chain incorporates four respiratory enzyme complexes arranged in a specific orientation in the inner mitochondrial membrane. The passage of electrons between these complexes is accompanied by pumping of protons across the membrane. In this content, the energy of electron flow is coupled to the pumping of protons across the inner mitochondrial membrane, which together produces an electrochemical gradient, the proton-motive force. The proton-motive force has two components: i) the transmembrane potential difference ($\Delta\Psi m$, being in the range of 150-180 mV, negative inside), and ii) the transmembrane proton concentration gradient (ΔpH). According to the chemiosmotic model, proposed by Peter Mitchell, the proton-motive force is capable of doing work which is used by F_o-F_1 ATP synthase to make ATP from ADP and P_i.

The mitochondrial F_o-F_1 ATP synthase is a reversible molecular machine. It is able to synthesize, and also to hydrolyze ATP (Boyer, 2002). The directionality of ATP synthase is conducted by the proton-motive force (Feniouk and Yoshida, 2008). As mentioned above, the proton-motive force consists of two components, but in the presence of sufficiently high concentration of inorganic phosphate, as it is the case *in vivo* (Wu et al., 2007), ΔpH is very small (Chinopoulos et al., 2009), so the directionality of F_o-F_1 ATP synthase is in general controlled by $\Delta\Psi m$. The value of $\Delta\Psi m$ at which F_o-F_1 ATP synthase shifts from ATP-forming to ATP-consuming is termed "reversal potential" (E_{rev_ATPase}) (Chinopoulos et al., 2011a).

The newly synthesized ATP is transported to the cytosol by adenine nucleotide translocase in exchange for ADP. This anti-porter works with a 1:1 stoichiometry across the inner mitochondrial membrane, and to be more exact, it utilizes the free forms of

ADP^{3-} and ATP^{4-} (however, F_o-F_1 ATP synthase utilizes the Mg^{2+} bound forms of ATP and ADP) (Senior et al., 2002). Together with ANT, phosphate translocase is also an essential membrane transporter of the inner mitochondrial membrane. It promotes symport of one P_i (*i.e.* $H_2PO_4^-$) and one H^+ into the matrix. As well as the ATP-ADP exchange is driven by proton-motive force, the symport of P_i and H^+ is also favored by transmembrane proton gradient. ANT is a reversible transporter, it can change the directionality. In mitochondria with compromised respiration, ATP could enter mitochondria by reverse operational ANT, and to be hydrolyzed by the F_o-F_1 ATP synthase. This process can maintain an appreciable proton-motive force in the absence of a functional respiratory chain (Scott and Nicholls, 1980). The value of ΔΨm at which ANT shifts from ATP-export to ATP-import is termed "reversal potential" (E_{rev_ANT}) (Metelkin et al., 2009).

In mitochondria with dis-functional ETC or in the absence of oxygen before becoming extramitochondrial ATP consumer there is one more possibility of ATP provision for reversal operating F_o-F_1 ATP synthase. ATP may be synthetised by matrix substrate-level phosphorylation. A decrease in ΔΨm (a shift toward more positive values) due to ETC inhibition or to an increase in the inner membrane permeability stops ATP synthesis and switches to ATP consumption, leading to bioenergetic failure in cells. In the mitochondrial matrix, two reactions are capable of substrate-level phosphorylation: the mitochondrial phosphoenolpyruvate carboxykinase (PEPCK) and the succinate-CoA ligase. Mitochondrial PEPCK is thought to participate in the transfer of the phosphorylation potential from the matrix to cytosol and *vice versa* (Lambeth et al., 2004). Succinate-CoA ligase is a mitochondrial matrix enzyme that catalyses the reversible conversion of succinyl-CoA and ADP or GDP to succinate and ATP or GTP (Johnson et al., 1998a). The enzyme is a heterodimer, being composed of an invariant α subunit encoded by *SUCLG1*, and a substrate-specific β subunit, encoded by either *SUCLA2* or *SUCLG2*. This dimer combination results in either an ADP-forming SUCL (A-SUCL, EC 6.2.1.5) or a GDP-forming SUCL (G-SUCL, EC 6.2.1.4). The β subunit thus determines the substrate specificity of the enzyme. Both β subunits are widely expressed in human tissues, with *SUCLG2* predominantly expressed in anabolic tissues such as liver, and *SUCLA2* in catabolic tissues such as brain and skeletal muscle (Johnson et al., 1998a; Lambeth et al., 2004). *SUCLG1* is ubiquitously expressed. The

widespread expression of both A-SUCL and G-SUCL in a wide range of animal species has been firmly established (Johnson et al., 1998a,b), and both enzymes are located in the matrix of mitochondria, where they could participate in the citric acid cycle.

The previous works of our group showed that when the ETC compromised and F_o-F_1 ATP synthase reverses, the mitochondrial membrane potential is still maintained, albeit at decreased levels. Even though the F_o-F_1 ATP synthase reverses, and pumps protons out of the matrix at the expense of ATP, ANT can function in forward mode as long as the matrix substrate-level phosphorylation is operational (Chinopoulos et al., 2010).

The directionality of F_o-F_1 ATP synthase is controlled by $\Delta\Psi m$, while F_o-F_1 ATP synthase itself is controlls the matrix ATP and ADP levels (Feniouk and Yoshida, 2008). Using thermodynamic assumptions and computer modeling (Chinopoulos et al., 2010), a so called "B space" (Figure 2) has been revealed within which F_o-F_1 ATP synthase reverses its directionality (*i.e.*, hydrolysis ATP), and still ANT operates in forward mode (*i.e.*, exports ATP from the matrix). For maintaining this "B space" it is known that it requires ATP supply generated by substrate-level phosphorylation, a mechanism that is independent from proton-motive force. Succinate-CoA ligase does not require oxygen for ATP production, and it is even activated during hypoxia (Phillips et al., 2009).

Experiments on *in situ* and isolated mitochondria also supported the conclusion from computation estimations (Chinopoulos et al., 2010), and it is obvious that ATP generated in reaction catalyzed by succinate-CoA ligase prevents mitochondria to become consumer of cytosolic ATP in the absence of oxygen or when the electron transport chain is impaired. Matrix substrate-level phosphorylation could be endogenous rescue machinery which, even though the mitochondria are depolarized, can maintain the $\Delta\Psi m$ at suboptimal level. Mitochondria could keep their integrity as long as matrix substrate-level phosphorylation is in operation, and provide ATP for the reversible reaction of the F_o-F_1 ATP synthase, but prevents ANT to reverse.

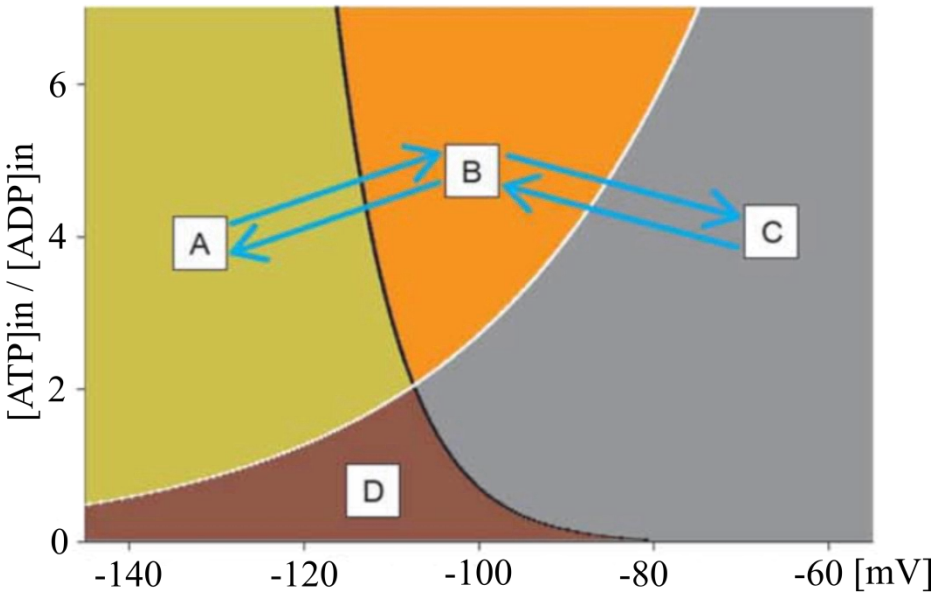

Figure 2. Computational estimation of E_{rev_ANT} and E_{rev_ATPase} as a function of [ATP]in/[ADP]in ratio. *Black line represents the E_{rev_ATPase}, white line the E_{rev_ANT}.*
A space: F_o-F_1 ATP synthase forward, ANT forward mode.
B space: F_o-F_1 ATP synthase reversed, ANT forward mode.
C space: F_o-F_1 ATP synthase reversed, ANT reversed mode.
D space: F_o-F_1 ATP synthase forward, ANT reversed mode – it is a theoretical consideration, and has never been experimentally reproduced.
SLP is operational in "B space", and may or may not operate in "A/C/D space". Blue arrows represent the reversible transition between the spaces.
(Reproduced from: Chinopoulos, 2011a)

The pioneering findings of our group showed that, in progressively depolarizing mitochondria, the ATP synthase and ANT may change directionality independently from one another (Chinopoulos et al., 2010). It was also demonstrated that when the electron transport chain is dysfunctional, provision of succinyl-CoA by the α-ketoglutarate dehydrogenase complex (KGDHC) is crucial for maintaining the functional succinate-CoA ligase yielding ATP (Kiss et al., 2013). In the irreversible reaction catalyzed by KGDHC, α-ketoglutarate, CoASH and NAD^+ is converted to succinyl-CoA, NADH and CO_2. After these findings the question was: What is the source of NAD^+ when the ETC is dysfunctional? It is common knowledge that NADH generated in the citric acid cycle is oxidized by complex I, and at the same time NAD^+

is recycled. In the absence of oxygen or when complexes are not functional, an excess of NADH in the matrix is expected. We presented that mitochondrial diaphorases and a finite pool of oxidizable quinones are the source of NAD^+ generated within the mitochondrial matrix during respiratory arrest caused by anoxia or dysfunctional ETC (Kiss et al., 2014). A diaphorase activity is attributed to a flavoprotein known as DT-diaphorase or NAD(P)H:quinone oxidoreductase (Ernster, 1958a,b). It appears to be a 2-electron transfer flavoprotein, which catalyzes the conversion of quinones into hydroquinones.

These finding were of importance to prove the relevance and functionality of SLP in mitochondria with compromised ETC. These ground experiments were of necessity before we considered the effect of itaconate on SLP.

In experiments with mitochondria to point out the relevance of SLP the so called "biosensor test" was used (Figure 3). To place respiration-impaired mitochondria withing space B or space C, its ΔΨm, matrix ATP/ADP ratio, reversal potential of F_o-F_1 ATP synthase and ANT are needed. To determine these parameters it is an extremely challenging experimental undertaking. The reversal potential of F_o-F_1 ATP synthase is more negative than that of the ANT (Chinopoulos et al., 2010). This means that whenever the ANT reverses, the ATP synthase works in reverse, too. In experiments insetead of measuring ΔΨm, matrix ATP/ADP ratio, E_{rev_ANT} and E_{rev_ATPase} at any given time, it is simpler and equally informative to examine the effect of ANT inhibitors on ΔΨm (estimated by fluorescence quenching of a cationic dye, which accumulates inside energized mitochondria) during ADP-induced respiration. Since one molecule of ATP^{4-} is exchanged for one molecule of ADP^{3-} by ANT, the exchange is electrogenic (Klingenberg, 2008). Therefore, during the forward mode of ANT (*i.e.*, transporting ADP^{3-} into and ATP^{4-} out of the matrix), abolition of its operation by a specific inhibitor leads to an increase in ΔΨm (*i.e.*, repolarization); wheres during the reverse mode of ANT (*i.e.*, transporting ATP^{4-} into and ADP^{3-} out of the matrix), the same condition leads to loss of ΔΨm (*i.e.*, depolarization). This "biosensor test" − the effect of ANT inhibitor on a safranin O or TMRM fluorescence reflecting ΔΨm − was successfully used in addressing the directionality of ANT during respiratory inhibition (Chinopoulos et al., 2010). By determining the directionality of ANT, at the same time, we could also decide on the operation or not of SLP.

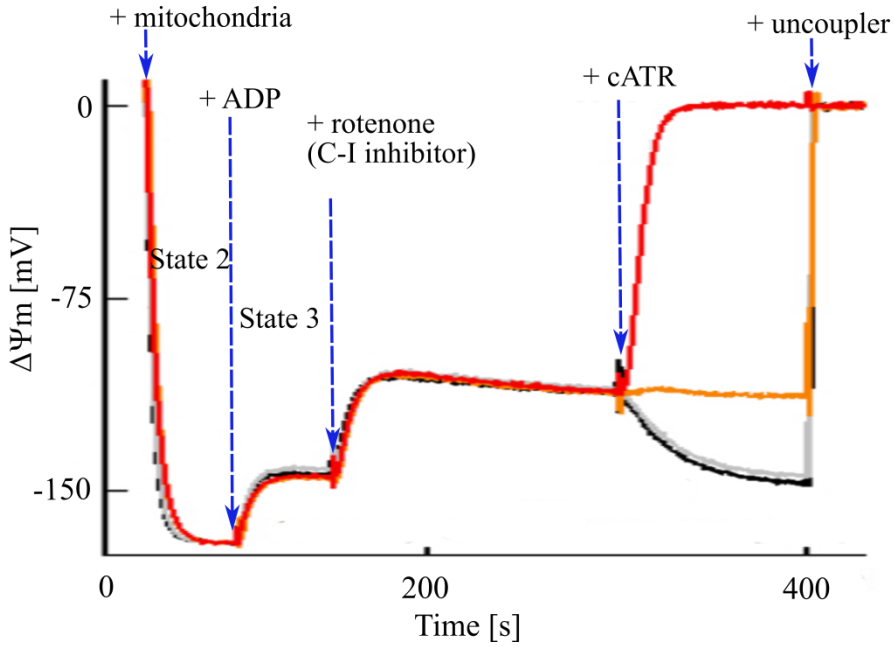

Figure 3. Schematic representation of the "biosensor test". *Fluorescence quenching of a cationic dye (safranin O), which accumulates inside energized mitochondria, reflects ΔΨm. State 2: mitochondrial polarization by substrates (substrates always present in the medium before addition of mitochondria). State 3: ADP-induced depolarization. After addition of complex I inhibitor, rotenone, the ETC is compromised, and ΔΨm is shifted toward more positive values, i.e., it is depolarized. During ETC arrest ΔΨm is supported by reversal of the ANT and/or reversal of F_o-F_1 ATP synthase. Addition of ANT inhibitor, carboxyatractyloside (cATR), can induce: repolarization (black trace) – implying forward operation of ANT, depolarization (red trace) – implying reversal operation of ANT, no change (orange trace) – implying ANT operating at its thermodynamic equilibrium. Addition of uncoupler (e.g. SF 6847) maximally depolarizes mitochondria, and it is used for ΔΨm calibration.*

2.5. Itaconic acid

Itaconic acid (2-methylidenebutanedioic acid, methylenesuccinic acid, CAS registry number: 97-65-4) is an unsaturated dicarboxylic acid. This organic compound plays an important role in immunity as well as in industrial biotechnology. Itaconic acid is produced from *cis*-aconitate by the extramitochondrial *cis*-aconitate decarboxylase, an enzyme encoded by the *cad1* gene in fungus *Aspergillus terreus* (Steiger et al., 2013).

Itaconic acid has a high potential as a biochemical compound, because the double bond of its methylene group makes it useful for polymer synthesis. It can be used as a monomer for the production of plethora of products including resins, plastics, paints and synthetic fibers (Okabe et al., 2009; Willke and Vorlop, 2001; Steiger et al., 2013), reviewed in (Cordes et al., 2015). Itaconic acid has been identified in a small number of metabolomic studies of mammalian tissue specimens, such as activated macrophages (Sugimoto et al., 2012), *Mycobacterium tuberculosis*-infected lung tissue (Shin et al., 2011), urine and serum samples (Kvitvang et al., 2011), and glioblastomas (Wibom et al., 2010). More recently, it has been shown that human and mouse macrophages produce itaconic acid from *cis*-aconitate through an enzyme exhibiting *cis*-aconitate decarboxylase activity, coded by the *cis*-aconitate decarboxylase 1 gene (previous name: immunoresponsive gene 1, *Irg1*) (Michelucci et al., 2013).

Some of the key features of itaconic acid are:

- It is of high interest to industry for its use in polymer synthesis − it is biotechnologically produced by the fungus *Aspergillus terreus*.
- It is generated through decarboxylation of the TCA cycle intermediate *cis*-aconitic acid by CAD in *Aspergillus terreus* and Acod1 in mammals.
- It plays an important role during inflammation and provides antimicrobial effects in macrophages.

2.5.1. Synthesis of itaconic acid

The first discoveries about itaconic acid root back into 1836. During distillation of citric acid Baup observed the formation of an unknown compound (Baup, 1836). A few years later the same substance was synthesized by decarboxylation of *cis*-aconitic acid. Crasso, the scientist who did the experiment, introduced the synthesized component as itaconic acid. The name itaconic acid represents an anagram of *cis*-aconitic acid (Turner, 1840; Cordes et al., 2015). Almost a century later, for the first time, Kinoshita found that itaconic acid was produced *in vivo*. He recognized that a filamentous fungus – which he descriptively named as *Aspergillus itaconicus* – was able to synthesize itaconic acid (Kinoshita, 1931; Steiger et al., 2013). To date it is known that, beside *Aspergillus species*, like *Aspergillus itaconicus* and *Aspergillus terreus* (Calam et al., 1939), itaconic acid is produced also by other fungi like *Ustilago zeae*

(Haskins et al., 1955) and *Ustilago maydis* (Haskins et al., 1955; Klement et al., 2012), as well as the yeast *Candida sp.* (Tabuchi et al., 1981) and *Rhodotorula sp.* (Kawamura et al., 1981). In a recent years, Sugimoto and coleagues (Sugimoto et al., 2012) discovered itaconic acid synthesis in mammalian immune cells, too.

2.5.2. Compartmentalization of itaconi acid synthesis in *Aspergillus terreus*

In 1957, Bentley and Thiessen proposed the itaconic acid formation pathway in fungus *Aspergillus terreus* (Bentley and Thiessen, 1957a,b). According to their hypothesis itaconic acid is formed from the citric acid cycle intermediate *cis*-aconitic acid by the the enzyme *cis*-aconitic acid decarboxylase, which is encoded by the gene *cad1*. Later, this pathway was confirmed by isotope tracing experiments with 14C and 13C labeled substrates (Bonnarme et al., 1995).

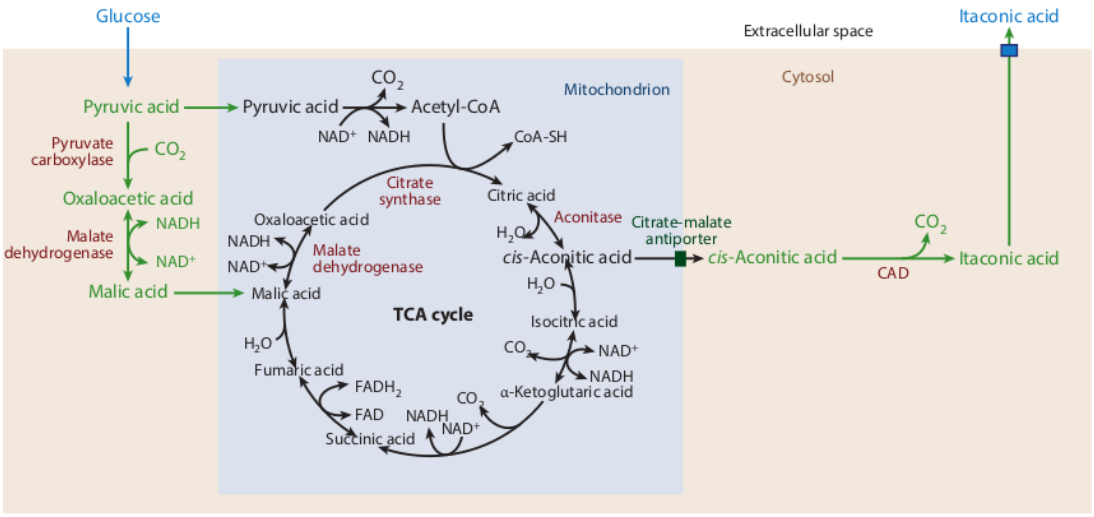

Figure 4. Compartmentalization of itaconic acid synthesis in Aspergillus terreus. *(Adopted from: Cordes et al., 2015)*

Starting from a sugar substrate, as a carbon source for itaconic acid production, the fungus takes up glucose from the extracellular environment, and processes it *via* glycolysis to pyruvate in the cytosol (Figure 4). Here the pathway splits. Pyruvic acid can enter the tricarboxylic acid cycle in the mitochondria either *via* acetyl-CoA or malic acid. During first steps of citric acid cycle, citrate and *cis*-aconitate are formed. In *Aspergillus terreus*, CAD is localized in the cytosol, and consequently, it is the location of itaconic acid production, too. Taken it into account, transport of *cis*-aconitic acid

from mitochodria to the cytosol is required. This relocation is done by citrate-malate antiporter (Jaklisch et al, 1991). However, the exact transport mechanism is still unknown. As a final step in itaconic acid biosynthesis, a secretion mechanism for itaconic acid is required because *Aspergillus terreus* accumulates itaconic acid in the extracellular environment (Steiger et al., 2013). Potential transporters involved are not yet known. The notion that itaconic acid is secreted in large amounts by *Aspergillus terreus* calls on hypothesizing that the compound is not further metabolized by this fungus and may have other functions.

2.5.3. Industrial production of itaconic acid

The discovery of itaconic acid has been of growing interest for industry because it can be used as a starting material for chemical synthesis of polymers (Okabe et al., 2009; Yu et al., 2011). The chemical structure of itaconic acid reveals its reactive methylene group which allows a self-polymerization to polyitaconic acid (Steiger et al., 2013). Therefore, itaconic acid is a potential replacement for crude oil-based products, and it is industrially used as a precursor for plastic polymer synthesis as well as for resins, lattices and fibers (Willke and Vorlop, 2001; Okabe et al., 2009; El-Imam and Du, 2014). Although the levels of itaconic acid which were reached with *Aspergillus terreus* are about 85 g/L, further optimizations are required by industrial companies. Compared to the industrial production of citric acid by *Aspergillus niger* where titers are measured about 200 g/L, the itaconic acid titers in industrial production are still low. Toward efficient itaconic acid production certain drawbacks of using filamentous fungi should be sort out.

The production of itaconic acid requires continuous oxygen supply. The process is strictly aerobic because low oxygen concentrations damage the mycelia and affect fungal metabolism (Gyamerah, 1995; Willke and Vorlop, 2001). This oxygen sensitivity could be reduced by gene engineered *Aspergillus terreus*. The hemoglobin gene of the aerobic bacterium *Vitreoscilla* expressed in *Aspergillus terreus* showed increased itaconic acid formation (Lin et al., 2004). Furthermore, the genetically modified strains showed a better recovery upon disturbed oxygen supply.

It has been reported that itaconic acid itself inhibits the grow of *Aspergillus terreus* and, in turn, decreases the itaconic acid production. This kind of suppression of

itaconic acid production could be overcome by using mutant strains that are itaconic acid resistant (Yahiro et al., 1995).

Another possible strategy to increase itaconic acid yields is in taking advantage of another host organism. As mentioned above, *Aspergillus niger* is known to produce 200 g/L of citric acid, a potential precursor in itaconic acid synthesis. The only obstacle is that *Aspergillus niger* lacks *cad1* gene. Although, after the *cad1* gene of *Aspergillus terreus* was engineered into *Aspergillus niger*, still itaconic acid titers were low compared to the synthetised citric acid. Many-fold increase in itaconic acid production was detected only after overexpression of mitochondrial transporter in combination with a plasma membrane transporter (Van der Straat et al., 2014).

Despite the efforts to optimize itaconic acid yields *Aspergillus terreus* is still the dominant production host.

2.5.4. Itaconic acid as an antimicrobial agent

Itaconic acid, together with other inflammatory metabolites and cytokines, performs an efficient immune response. On the contrary, invading pathogens aren't that *naïve*, and have developed a defense strategy against itaconic acid, degrading and detoxifying its antimicrobial effects (Ménage et al., 2014; Sasikaran et al., 2014).

Antimicrobial activity of itaconic acid is administered through action on pathogen metabolism (Figure 5). Modes of these actions are:

i) inhibition of isocitrate lyase, the key enzyme of the glyoxylate shunt,

ii) inhibition of methylisocitrate lyase, the enzyme of 2-methylcitrate cycle,

iii) inhibition of propionyl-CoA carboxylase, the enzyme of citramalate cycle.

The glyoxylate shunt allows many bacteria to utilize acetyl-CoA generating carbon sources such as fatty acids or cholesterol for biomass production under glucose-limiting conditions (Kumar R. 2009). As an example, *Salmonella enterica* and *Mycobacterium tuberculosis* depend on this metabolic mechanism during persistence within macrophages (McKinney et al., 2000; Fang et al., 2005; Kumar R. 2009).

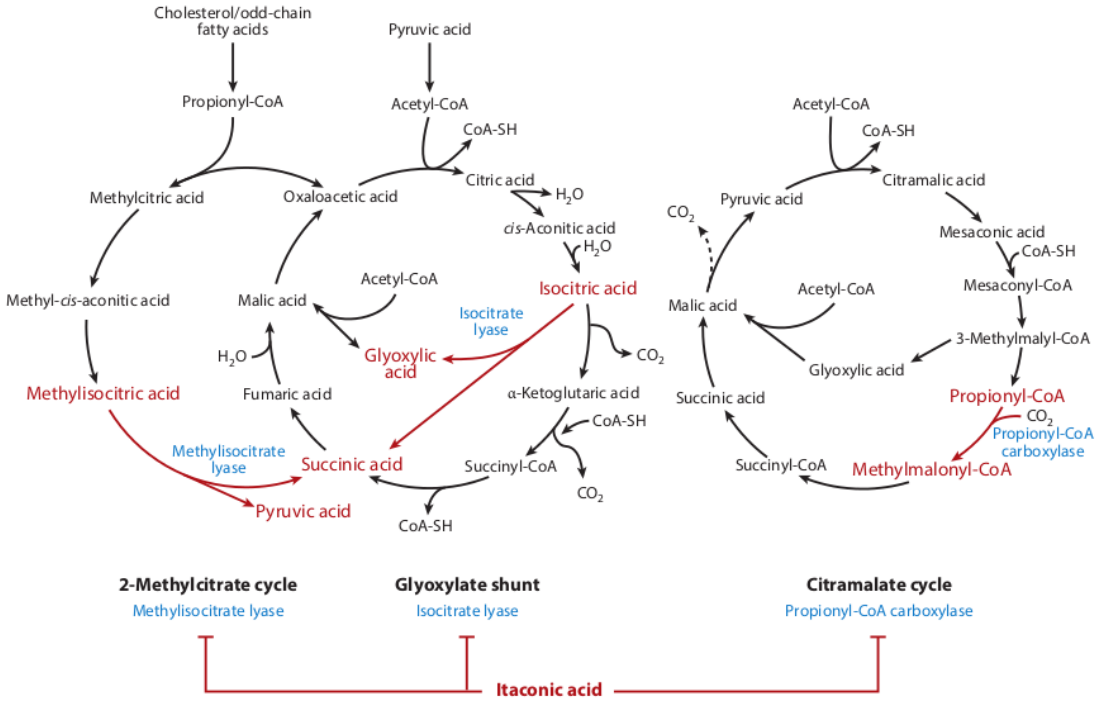

Figure 5. Antimicrobial activity of itaconic acid. Action of itaconic acid on pathogen metabolism. *In blue: eznyzmes inhibited by itaconic acid; in red: inhibited biochemical pathways. (Adopted from: Cordes et al., 2015)*

The glyoxylate shunt, like the citric acid cycle, begins with the condensation of acetyl-CoA and oxaloacetate to form citrate, which is then isomerized to isocitric acid. Instead of being decarboxylated, isocitric acid is converted by isocitrate lyase into succinic acid and glyoxylate. In the next step malic acid is produced by malate synthase condensing acetyl-CoA with glyoxylate (Sharma et al., 2000; Dunn et al., 2009). In the final step of glyoxylate shunt, malate is oxidized to oxaloacetate, as in the citric acid cycle.

Itaconic acid inhibits isocitrate lyase, the key enzyme of glyoxylate shunt. It functions as a competitive inhibitor, competing with succinic acid (McFadden et al., 1971), presumably by binding to the active site of the enzyme. The glyoxylate shunt with its exclusive presence in microbes, offers possibility for a potential drug target (Muñoz-Elías and McKinney, 2006).

In addition to isocitrate lyase, itaconic acid also inhibits other enzymes of invading pathogens. When glucose availability is limited, invading pathogens, such as *Mycobacterium tuberculosis*, use cholesterol from the host as a carbon source (Pandey

and Sassetti, 2008; Russell et al., 2010). During cholesterol degradation, in the last step, propionyl-CoA is produced. Since propionyl-CoA is toxic for the pathogens (Berg et al., 2002; Upton and McKinney, 2007), they detoxify this compound to succinic acid and pyruvic acid in the 2-methylcitrate cycle. The key enzyme of this cycle is methylisocitrate lyase – an enzyzme very similar to isocitrate lyase –, which converts methylisocitric acid to pyruvic acid and succinic acid, and is also inhibited by itaconic acid (Van der Geize et al., 2007). Itaconic acid exhibits a dual inhibition on bacterial enzymes: first, inhibition of methylisocitrate lyase activity cancels detoxification of propionic acid; second, the inhibition of isocitrate lyase leads to the inhibiton of the bacterial biomass generation through the glyoxylate shunt. This means that itaconic acid plays a prominent role as an endogenous antimicrobial compound (Michelucci et al., 2013).

Beside the above-mentioned pathways – glyoxylate shunt and 2-methylcitrate cycle – itaconic acid also inhibits propionyl-CoA carboxylase, an enzyme that carboxylizes propioyl-CoA to methylmalonyl-CoA in the citramalate cycle (Berg et al., 2002). This pathway is proposed to the proteobacterium *Rhodospirillum rubrum*, which lacks isocitrate lyase activity. The inhibition of propionyl-CoA carboxylase by itaconic acid leads to an inhibition of acetic acid and propionic acid assimilation in cell extracts of this bacterium.

2.5.5. Itaconic acid in mammalian cells

Strelko and colleagues reported about itaconic acid as a novel mammalian metabolite that most likely plays a role in macrophages during immune responses (Strelko et al., 2011). Another group also discovered itaconic acid in the extracellular environment of mammalian cells – as a metabolite of LPS-activated macrophages –, but did not discuss its biological relevance (Sugimoto et al., 2012).

Following the discovery of itaconic acid in mammalian immune cells, its biosynthesis pathway was also revealed. Experminets using LPS-activated macrophages, incubated with uniformly labeled [U-13 C6]glucose, revealed that mammalian cells produce itaconic acid through decarboxylation of the TCA cycle intermediate *cis*-aconitic acid (Strelko et al., 2011; Michelucci et al., 2013). This is the same metabolic pathway as described for *Aspergillus terreus*. Applying sequence

homology search for *Aspergillus* CAD, the Acod1 enzyme was revealed, as a CAD homologue in mammals (Michelucci et al., 2013).

Acod1 upregulation was observed in different type of cells: murine macrophages infected with *Mycobacteria* (Basler et al., 2006) or *Salmonella enterica* (Michelucci et al., 2013) as well as in LPS-stimulated bone marrow-derived dendritic cells (Hoshino et al., 2002); it was detected in human fetal peripheral blood mononuclear cells (PBMCs) and LPS-stimulated adult PBMCs (Xiao et al., 2011) as well as in endotoxin-activated PBMC-derived macrophages (Michelucci et al., 2013); murine microglial cells – macrophage analogues of the central nervous system –, performed *Acod1* upregulation after being infected *in vivo* with *Toxoplasma gondii* (Li et al., 2006) and *in vitro* after LPS stimulation (Thomas et al., 2006); in the lung tissue of mice during the early phase of influenza A virus infection (Preusse et al., 2013) and in chickens infected with Marek's disease (Smith et al., 2011). Increased *Acod1* expression was detected after infection with neurotropic viruses. In this analysis, *Acod1* expression was detected in granule cell neurons of the cerebellum and in cortical neurons from the cerebral cortex (Cho et al., 2013). Independently from bacterial or viral infections, an upregulation of *Acod1* expression has been detected in the early events leading to implantation in the pregnant uterus (Terakawa et al., 2011).

Experiments with MitoTracker Green FM, a fluorescent compound that accumulates specifically in mitochondria, revealed that Acod1 is localized to the mitochondria (Degrandi et al., 2009). It is in contrast to its localization in *Aspergillus terreus*, where the enzyme synthesizing itaconate, CAD, is placed to the cytosol.

Although the applications of itaconic acid and its derivatives extend to dental, ophthalmic, and drug delivery fields (Okabe et al., 2009), and in complexation with benzylammonium it is used to prepare water soluble coating for food packaging to reduce bacteria contamination, it does not enter the food chain to an appreciable degree. Still, it was shown to be extensively metabolized when administered *per os* to cats, dogs and murine animals (Booth et al., 1952; Adler et al., 1957).

There are evidences about itaconic acid affecting energy metabolism. Itaconic acid inhibits rat liver phosphofructokinase-2, a regulatory enzyme of the glycolytic pathway. Due to the inhibition of the glycolytic pathway, it has been shown that itaconic acid suppresses the synthesis of fatty acids from glucose. In rats, an itaconic acid-

enriched diet leads to a reduced visceral fat accumulation; therefore, itaconic acid could play a role in controlling obesity (Sakai et al., 2004). In addition to the inhibition of glycolysis, itaconic acid has an inhibitory effect on succinate dehydrogenase (SDH) (Booth et al., 1952; Dervartanian and Veege; 1964). This enzyme complex binds to the inner mitochondrial membrane and oxidizes succinic acid to fumaric acid as part of the TCA cycle and in turn reduces FAD to FADH2, which feeds into the electron transport chain. Apart from SDH inhibition, itaconate could contribute to the accumulation of succinic acid. In the review by Mills and O'Neill, two other possible sources are discussed: i) the first source is an increased glutamine uptake in LPS-activated macrophages and subsequent anaplerosis of α-ketoglutaric acid into the TCA cycle, which may lead to increased succinic acid production; ii) the second source is based on γ-aminobutyric acid (GABA) production; GABA can then be a substrate for succinic acid synthesis *via* transamination (Mills and O'Neill, 2014).

2.5.6. The pathway of itaconate metabolism in murine liver mitochondria

More than 50 years ago it was reported, by Adler and colleagues that exogenously added itaconic acid to isolated mitochondria is oxidized as most members of the citric acid cycle (Adler et al., 1957). The same group elucidated the pathway of itaconic acid metabolism towards pyruvate and acetyl-CoA, (Wang et al., 1961); however, at that time, the identity of succinate-CoA ligase (referred to as "succinate-activating enzyme", or "P enzyme"), and its role in substrate-level phosphorylation was not yet revealed (Sanadi et al., 1954; Labbe et al., 1965; Ottaway et al., 1981).

Based on these earlier findings we merged itaconic acid metabolism with the part of TCA cycle and related metabolic reactions that involve SLP. As shown in Figure 6, itaconate (shown in bold) arises from *cis*-aconitate, an intermediate of the aconitase reaction, but only in tissues where *cis*-aconitate decarboxylase is expressed (Xiao et al., 2011). In the fungus *Aspergillus terreus*, CAD is an extramitochondrial protein (Steiger et al., 2013); in mammalian cells, an iron-responsive element binding protein exhibiting aconitase activity has been found in the cytosol (Haile et al., 1992), however, in cells of macrophage lineage (where itaconate is formed) *cis*-aconitate decarboxylase associates to mitochondria (Degrandi et al., 2009). *cis*-aconitate may arise from either isocitrate or citrate, since the reaction catalyzed by aconitase is reversible. Exogenously

administered itaconate would be further metabolized only after entry into the mitochondria. Such entry is expected to occur through the dicarboxylate carrier (SLC25A10), although, to the best of our knowledge, this has not been verified.

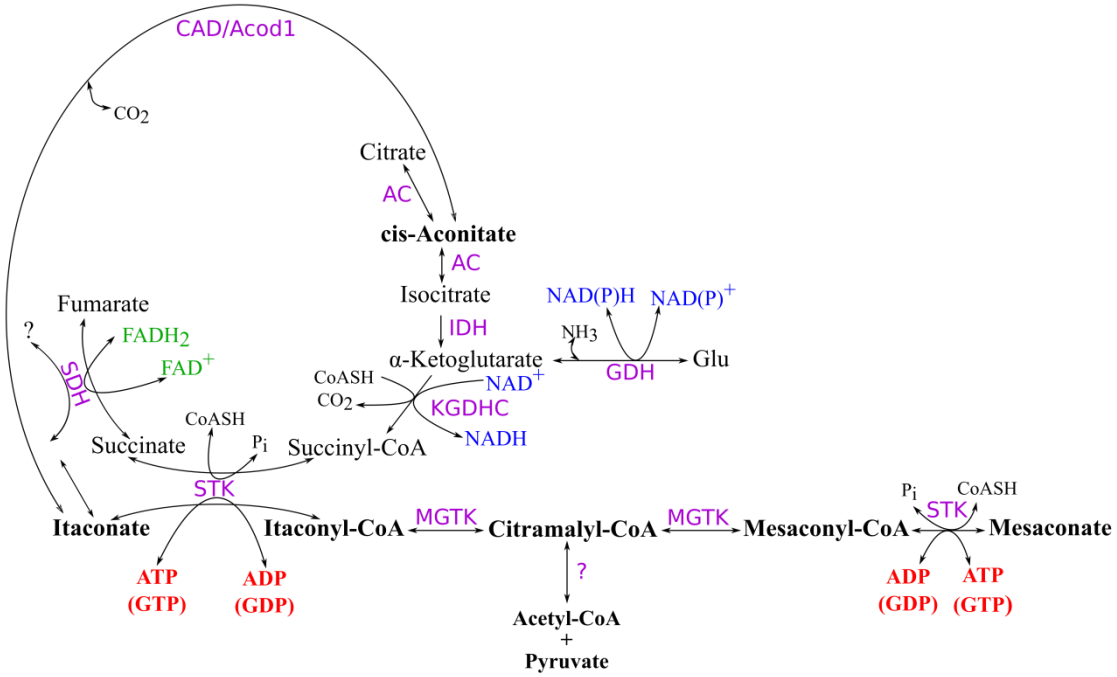

Figure 6. Schematic representation of itaconate and mesaconate metabolism in relation to a segment of the TCA cycle and reactions involved in SLP. *SDH: succinate dehydrogenase; STK: succinate thiokinase (succinate-CoA ligase); KGDHC: α-ketoglutarate dehydrogenase complex; GDH: glutamate dehydrogenase; MGTK: methylglutaconase (methylglutaconyl-CoA hydratase); CAD/Acod1: cis-aconitate decarboxylase; AC: aconitase (aconitate hydratase); IDH: isocitrate dehydrogenase.*

In the mitochondrial matrix, itaconate could weakly inhibit succinate dehydrogenase in a competitive manner (Booth et al., 1952; Adler et al., 1957; Haile et al., 1992; Xiao et al., 2011). The work of Adler *et al.* showed that itaconate would also become oxidatively catabolized in the citric acid cycle in a malonate-sensitive manner (Adler et al., 1957), however, due to the lack of hydrogen on the α-carbon of itaconate, a double bond cannot be formed; therefore it cannot be processed by SDH as such. Two

possibilities by which itaconate is converted to products suitable for oxidation by the SDH could be envisaged: i) saturation of itaconate to methylsuccinate is the most likely scenario, in view of the fact that methylsuccinate is known to be processed by SDH (Franke et al., 1957; Dervartanian and Veeger, 1964); ii) itaconate hydroxylation yielding hydroxymethyl-succinate is also a viable theoretical possibility, but to the best of our knowledge this has not been addressed. A possible decarboxylation or isomerisation of itaconate would yield products that cannot be further metabolized by SDH.

On the other hand, in acetone extracts of murine liver mitochondria, itaconate metabolism was shown to occur extensively in the presence of ATP, Mg^{2+} and CoASH (Adler et al., 1957). Furthermore, in intact liver mitochondria and in the presence of ATP and Mg^{2+} but absence of oxygen, itaconate became thioesterified to itaconyl-CoA which was later converted to citramalyl-CoA through methylglutaconyl-CoA hydratase (also known as methylglutaconase, MGTK) (Abramov and Duchen, 2005). Citramalyl-CoA could be further converted to either mesaconyl-CoA by MGTK, or to acetyl-CoA and pyruvate (Adler et al., 1957; Wang, S. F. et al., 1961). Mesaconyl-CoA can lose the CoASH in a reaction catalyzed by succinate-CoA ligase, forming mesaconate. This also means that mesaconate would exhibit similar effects on SLP as itaconate; however, mesaconate is much less potent than itaconate (Adler et al., 1957), probably because of a lower affinity of succinate-CoA ligase for mesaconate than for itaconate.

3. OBJECTIVES

In one of the earlier works, our group highlighted the critical importance of matrix substrate-level phosphorylation during respiratory arrest (Chinopoulos et al., 2010). In the absence of oxygen or when the electron transport chain is impaired, matrix substrate-level phosphorylation is the only means of high-energy phosphates production in mitochondria. Mitochondrial substrate-level phosphorylation is almost exclusively attributable to an citric acid cycle enzyme, succinate-CoA ligase, which catalyzes the reversible conversion of succinyl-CoA and ADP (or GDP) to coenzyme A, succinate and ATP (or GTP) (Johnson et al., 1998a). Thanks to matrix substrate-level phosphorylation, even though the electron transport chain is compromised and F_o-F_1 ATP synthase reverses – instead of ATP synthesis it hydrolysis ATP –, the mitochondrial membrane potential is maintained, albeit at decreased levels (Chinopoulos et al., 2010). This process prevents mitochondria from becoming cytosolic ATP consumers (Chinopoulos, 2011a,b).

We assumed that itaconic acid exerts bioenergetic effects on adenine (or guanine) nucleotide production in the mitochondrial matrix *via* succinate-CoA ligase.

We set as an aim:

- to investigate specific bioenergetic effects of increased itaconate production mediated by LPS-induced stimulation of *cis*-aconitate decarboxylase 1 in macrophages;
- to investigate the dose-dependent effect of exogenously added itaconate to isolated liver mitochondria, under defined metabolic conditions to reveal the mechanism(s) of itaconate on SLP.

4. METHODS

4.1. Animals

Mice were of C57Bl/6 background. The animals used in our study were of both sexes and between 2 and 3 months of age. Mice were housed in a room maintained at 20-22°C on a 12 hours light-dark cycle with food and water available *ad libitum*. All experiments were approved by the Animal Care and Use Committee of the Semmelweis University (Egyetemi Állatkísérleti Bizottság).

4.2. Isolation of mitochondria

Liver mitochondria from all animals were isolated as described in Tyler and Gonze, 1967, with minor modifications detailed in Chinopoulos et al., 2010. Following cervical dislocation, the liver was rapidly removed, minced, washed and homogenized using a glass/PTFE Potter-Elvehjem tissue grinder in ice-cold isolation buffer containing, in mM: mannitol 225, sucrose 75, HEPES 5 (free acid), EGTA 1 and 1 mg/ml bovine serum albumin (BSA, essentially fatty acid-free), pH 7.4 adjusted with Trizma® (Sigma-Aldrich, St. Louis, MO, USA). The homogenate was centrifuged at 3,000 g for 10 min; the upper fatty layer of the supernatant was aspirated and the pellet was discarded, then the remaining supernatant was centrifuged at 10,000 g for 10 min; this step was repeated once. At the end of the third centrifugation, the supernatant was discarded, and the pellet was suspended in 100 ml of the same buffer with 0.1 mM EGTA.

Protein concentration was determined using the bicinchoninic acid assay, and calibrated using bovine serum standards (Smith et al., 1985) using a Tecan Infinite® 200 PRO series plate reader (Tecan Deutschland GmbH, Crailsheim, Germany). Yields were typically 0.4 ml of ~60 mg/ml per mouse liver.

4.3. Determination of membrane potential (ΔΨm) in isolated liver mitochondria

ΔΨm of isolated mitochondria (1 mg per 2 ml of medium containing, in mM: KCl 8, K-gluconate 110, NaCl 10, HEPES 10, KH_2PO_4 10, EGTA 0.005, mannitol 10, $MgCl_2$ 1, substrates as indicated in the legends, 0.5 mg/ml bovine serum albumin [fatty acid-free], pH 7.25 and 5 μM safranine O) was estimated fluorimetrically with safranine O (Åkerman and Wikström, 1976). Traces obtained from mitochondria were calibrated to millivolts by voltage-fluorescence calibration curve. To this end, safranine O

fluorescence was recorded in the presence of 2 nM valinomycin and stepwise increasing [K^+] (in the 0.2-120 mM range), which allowed calculation of ΔΨm by the Nernst equation, assuming a matrix [K^+] = 120 mM (Chinopoulos et al., 2010). Fluorescence was recorded in a Hitachi F-7000 spectrofluorimeter (Hitachi High Technologies, Maidenhead, UK) at a 5 Hz acquisition rate, using 495 and 585 nm excitation and emission wavelengths, respectively, or at a 1 Hz rate using the O2k-Fluorescence LED2-Module of the Oxygraph-2k (Oroboros Instruments, Innsbruck, Austria) equipped with an LED exhibiting a wavelength maximum of 465 ± 25 nm (current for light intensity adjusted to 2 mA, *i.e.*, level 4) and an <505 nm short-pass excitation filter (dye-based, filter set Safranin). Emitted light was detected by a photodiode (range of sensitivity: 350-700 nm), through an >560 nm longpass emission filter (dye-based). Experiments were performed at 37°C. Safranine O is known to exert adverse effects on mitochondria if used at sufficiently high concentrations (*i.e.* above 5 μM, discussed elsewhere) (Kiss et al., 2014). However, for optimal conversion of the fluorescence signal to ΔΨm, a concentration of 5 μM safranine O is required, even if it leads to diminishment of the respiratory control ratio by approximately one unit (not shown). Furthermore, the non-specific binding component of safranine O to mitochondria (dictated by the mitochondria/safranine O ratio) was within 10% of the total safranine O fluorescence signal, estimated by the increase in fluorescence caused by the addition of a detergent to completely depolarized mitochondria (not shown). As such, it was accounted for, during the calibration of the fluorescence signal to ΔΨm.

4.4. Mitochondrial respiration

Oxygen consumption was estimated polarographically using an Oxygraph-2k. Liver mitochondria (2 mg) were suspended in 4 ml incubation medium, the composition of which was identical to that for ΔΨm determination. Experiments were performed at 37°C. Oxygen concentration and oxygen flux ($pmol \cdot s^{-1} \cdot mg^{-1}$; negative time derivative of oxygen concentration, divided by mitochondrial mass per volume and corrected for instrumental background oxygen flux arising from oxygen consumption of the oxygen sensor and back-diffusion into the chamber) were recorded using DatLab software (Oroboros Instruments).

4.5. Cell cultures

BMDMs preparation: Bone marrow cells from mice were first cultured in Minimum Essential Medium α (Life Technologies, Carlsbad, CA, USA) complemented with 10% fetal bovine serum (Life Technologies), 2 mM L-glutamine (Sigma-Aldrich, St. Louis, MO, USA), 1% penicillin/streptomycin (Sigma) and 10 mM HEPES in the presence of 10 ng/ml mouse M-CSF (macrophage colony-stimulating factor) (PeproTech EC Ltd., London, UK). After 2 days, non-adherent cells were plated on 9 cm diameter petri plates (Gosselin SAS, France) at a density of 5-10×10^6 cells/plate and cultured in the same medium but M-CSF was supplied as a 10% conditioned medium from CMG14-12 cells. Medium/cytokine was changed in every two days.

TIPMs preparation: Thioglycollate-induced peritoneal macrophages were obtained by lavage of the peritoneal cavity of C57BL/6 mice which were injected 3 days previously with 1 ml of a medium containing 4.38 mM sodium thioglycollate (Liofilchem, s.r.l., Abruzzi, Italy). The cells were plated and cultured similarly as for the BMDMs.

RAW-264.7 cells preparation: RAW-264.7 cells were cultured in RPMI 1640 medium containing L-glutamine (Lonza, Basel, Switzerland), supplemented with 10% fetal bovine serum (Life Technologies) and 1% penicillin/streptomycin (Sigma). The medium was changed every 2 days. Cells were plated at either 250-500,000 cells/ml on 10 cm bacterial petri dishes (Bovimex, Székesfehérvár, Hungary) for Western blot analysis (see below), or at 30,000 or 90,000 cells/ml on 8-well chambered cover glass (Lab-Tek, Nalge Nunc, Penfield, NY, USA) for image analysis (see below). Eight hours after plating, fresh medium with or without ultrapurified LPS (InvivoGen, Toulouse, France) was added and the cells were cultured for additional 12 hours before cell lysis or imaging.

COS-7 cells preparation: COS-7 cells were grown on 175 cm^2 flasks in DMEM with glutamine, 10% FCS and 1% streptomycin-penicillin. On reaching confluence (15-17×10^6 cells/flask), cultures were harvested by trypsinization and were transfected by electroporation according to the manufacturer's instructions (Amaxa Inc., Gaithersburg, MD, USA).

4.6. Mitochondrial membrane potential (ΔΨm) measurement in cultured BMDM and RAW-264.7 cells

For ΔΨm, cells in 8-well chambered cover glasses (Lab-Tek, Nunc) were loaded with 180 nM tetramethylrhodamine methyl ester (TMRM) (Life Technologies) for 1hour at 37^{o}C in a buffer containing, in mM: NaCl 120, KCl 3.5, $CaCl_2$ 1.3, $MgCl_2$ 1.0, HEPES 20, glucose 15, pH 7.4. Prior to imaging the chambered cover glass was mounted into a temperature controlled (34^{o}C) incubation chamber on the stage of an Olympus IX81 inverted fluorescence microscope equipped with a ×20 0.75 NA air lens, a Bioprecision-2 *xy*-stage (Ludl Electronic Products Ltd., Hawthorne, NY) and a 75W xenon arc lamp (Lambda LS, Sutter Instruments, Novato, CA, USA). Time lapse epifluorescence microscopy was carried out without super fusion in the medium mentioned above. For TMRM, a 525/40 nm exciter, a 555LP dichroic mirror and a 630 band pass (bandwidth: 75 nm) emitter (Chroma Technology Corp., Bellows Falls, VT) were used. Time lapses of 1342×1024 pixels frames (digitized at 12 bit, with ×4 binning, 250 msec exposure time) were acquired (once every 90 s) using an ORCA-ER2 cooled digital CCD camera (Hamamatsu Photonics, Hamamatsu, Japan) under control of MetaMorph 6.0 software (Molecular Devices; Sunnyvale, CA, USA). For fluorescein-tagged siRNA or scrambled siRNA (see below) a 488/6 nm exciter, a 505LP dichroic mirror and a 535/25 band pass emitter (Chroma) were used. A time lapse of 1342×1024 pixels frames (digitized at 12 bit, with ×1 binning, 500 ms exposure time) was acquired once at the beginning of the experiments in order to identify the transfected cells.

4.7. Image analysis

Image analysis was performed in Image Analyst MKII (Novato, CA). Due to significant migration of cells during the measurements, first time series of images were maximum intensity projected into a single frame (pixel by pixel) and regions of interests (ROIs) were subsequently selected by an automated algorithmic tool of the software. This tool uses a random process to find the boundaries of a bright object (in our case, a migrating cell); upon selecting the middle of the bright object (using a pointer), the tool calculates the mean intensity in the vicinity of the pointer, then it extends the selection for the similarly bright pixels, until the variance of the pixel intensities does not reach a

preset threshold. The ROIs were subsequently assigned to individual cells and TMRM intensities corresponding to individual cells were plotted over time.

4.8. Measurement of *in situ* mitochondrial oxidation and glycolytic activity

Real-time measurements of oxygen consumption rate (OCR), reflecting mitochondrial oxidation, and extracellular acidification rate (ECAR), considered as a parameter of glycolytic activity, were performed on a microfluorimetric XF96 Analyzer (Seahorse Bioscience, North Billerica, MA, USA) as previously described (Gerencser et al., 2009). Cells were seeded 1-2 days before measurement in Seahorse XF96 cell culture microplates at ~25,000-50,000 cells/well density and were treated with 0, 10, 100 and 5,000 ng/ml ultrapurified LPS (InvivoGen, Toulouse, France) for 12 hours. One hour before measurement, growth media was changed to XF assay media according to manufacturer's instructions. After 1 hour incubation in assay medium, O_2 tension and pH values were detected and OCR/ECAR values were calculated by the XF96 Analyzer software. During the measurement, 20-26 µl of testing agents prepared in assay media were then injected into each well to reach the desired final working concentration. Data were normalized to total protein content, measured with BCA protein assay kit (Thermo Scientific, Rockford, IL, USA).

4.9. Western blot analysis

Five million cells that were plated on 10 cm bacterial petri dishes were harvested by trypsinization, washed in phosphate-buffered saline, solubilised in RIPA buffer containing a cocktail of protease inhibitors (Protease Inhibitor Cocktail Set I, Merck Millipore, Billerica, MA, USA) and frozen at –80^{o}C for further analysis. Frozen pellets were thawed on ice, their protein concentration was determined using the bicinchoninic acid assay as detailed above and separated by sodium dodecyl sulfate-polyacrylamide gel electrophoresis (SDS-PAGE). Separated proteins were transferred to a methanol-activated polyvinylidene difluoride membrane. Immunoblotting was performed as recommended by the manufacturers of the antibodies. Rabbit polyclonal anti-Acod1 (ab122624, Abcam, Cambridge, UK 1:500 dilution), rabbit polyclonal anti-Acod1 (ab1238627, Abcam, 1:500 dilution), mouse monoclonal anti-FLAG (ab18230, Abcam, UK 1:500 dilution) and mouse monoclonal anti-β actin (ab6276, Abcam, 1:5,000 dilution) primary antibodies were used. Immunoreactivity was detected using the

appropriate peroxidase-linked secondary antibody (1:5,000, donkey anti-rabbit or donkey anti-mouse; Jackson Immunochemicals Europe Ltd, Cambridgeshire, UK) and enhanced chemiluminescence detection reagent (ECL system; Amersham Biosciences GE Healthcare Europe GmbH, Vienna, Austria).

4.10. Fluorescein-tagged siRNA and cell transfections

The ON-TARGETplus SMARTpool containing 4 different siRNA sequences, all specific to murine *Acod1* and the corresponding nontargeting control (scrambled siRNA), were designed by Thermo Scientific Dharmacon and synthesized by Sigma-Aldrich. All 4 siRNAs and the scrambled siRNA sequences were manufactured to contain a fluorescein tag on the 5' end of the sense strand only. RAW264.7 cells were transfected with 100 nM of either siRNA or scrambled siRNA using Lipofectamine 2000 (Invitrogen, Carlsbad, CA, USA) according to the manufacturer's instructions, 12 hours before a subsequent treatment with 5 μg/ml LPS, or vehicle. One day prior to transfections, cells were plated in their regular medium (see above) in the absence of antibiotics. As such, lipofectamine and siRNA (or scrambled siRNA) were present for 24 hours and LPS for 12 hours prior to any subsequent measurements.

4.11. *Acod1*-FLAG plasmid transfections

pCMV6-FLAG-*Acod1* overexpressing plasmid (4.2 μg, *Mus musculus cis*-aconitate decarboxylase 1 gene transfection-ready DNA, OriGene) was transfected into 5×10^6 RAW-264.7 or COS-7 cells cultures cells using Lipofectamine 2000 (Invitrogen) and further incubated for 24-48 hours.

4.12. Immunocytochemistry

RAW-264.7 cell cultures were transfected with the pCMV6-FLAG-*Acod1* overexpressing plasmid for at least 24 hours in Opti-MEM 1 (reduced serum medium without antibiotics, suitable for transfection experiments) at 37^{o}C in 5% CO_2. Prior to fixation, cells were treated with 1 μM Mitotracker Orange (MTO) for 5 min. Subsequent immunocytochemistry of the cultures was performed by fixing the cells with 4% paraformaldehyde in PBS for 20 min, followed by permeabilization by 0.1% TX-100 (in PBS) for 10 min and several washing steps in between with PBS at room temperature. Cultures were treated with 10% donkey serum overnight at 4^{o}C followed by bathing in 1% donkey serum and anti-FLAG antibody (ab18230, Abcam, 1:500

dilution) for 1 hour at room temperature. Cells were subsequently decorated by using the appropriate Alexa 492-linked secondary antibody (1:4,000, donkey anti-mouse; Jackson Immunochemicals Europe Ltd, Cambridgeshire, UK) in the presence of 1% donkey serum. Cells were visualized using the imaging setup mentioned above.

4.13. Determination of SDH activity

The activity of SDH in isolated liver mitochondria was determined by spectrophotometric assay as described by Saada et al., 2004.

4.14. Statistics

Data are presented as averages ± SEM. Significant differences between two groups were evaluated by Student-s t-test; significant differences between 3 or more groups were evaluated by 1-way ANOVA followed by Tukey's or Dunnett's *post hoc* analysis. $P < 0.05$ was considered statistically significant. If normality test failed, ANOVA on Ranks was performed. Wherever single graphs are presented, they are representative of at least 3 independent experiments.

4.15. Reagents

Standard laboratory chemicals and itaconic acid were from Sigma-Aldrich. SF 6847 and atpenin A5 were from Enzo Life Sciences (ELS AG, Lausen, Switzerland). Carboxyatractyloside (cATR) was from Merck (Merck KGaA, Darmstadt, Germany). KM4549SC (LY266500) was from Molport (SIA Molport, Riga, Latvia). LPS was from InvivoGen (InvivoGen Inc, Toulouse, France). Mitochondrial substrate stock solutions were dissolved in bidistilled water and titrated to pH 7.0 with KOH. ADP was purchased as a K^+ salt of the highest purity available (Merck) and titrated to pH 6.9.

5. RESULTS

5.1. The effect of LPS on matrix SLP in macrophage cells

As mentioned earlier, cells of macrophage lineage upon LPS induction express Acod1, an enzyme catalyzing the decarboxylation of *cis*-aconitate to itaconate (Strelko et al., 2011; Michelucci et al., 2013). Prior to investigating the effect of LPS on matrix substrate-level phosphorylation in macrophage cells, we tried to establish the conditions in which we observe Acod1 expression.

We investigated three types of macrophages:

i) murine bone marrow-derived macrophages (BMDM),

ii) macrophage-like RAW-264.7 cells,

iii) murine thioglycollate-induced peritoneal macrophages (TIPM).

As shown in Figure 7A, BMDM, RAW-264.7 and TIPM cells were challenged by different concentrations of LPS (0, 10, 100 and 5,000 ng/ml) for 12 hours. Acod1 expression was tested by Western blot. Two different antibodies were used, each rose against different epitopes of the Acod1 protein. Cell types, concentration range and time frame for LPS treatment was chosen according to experimental data published elsewhere, using LPS in the low nano- to micromolar range, for 1-24 hours (Xaus et al., 2000; Hoebe et al., 2003; Hoentje. et al., 2005; Kimura et al., 2009; Strelko et al., 2011; Liu et al., 2012; Xu et al., 2012; Michelucci et al., 2013). Equal loading of the wells was verified by probing for β-actin. As shown in the scanned blots of Figure 7A, Acod1 expression was detected in BMDM and RAW-264.7 cells, but not in TIPM cells. Excellent agreement among results was obtained from the two different anti-Acod1 antibodies. Perhaps for TIPM cells a shorter or longer than 12 hours LPS treatment is required to induce *Acod1*. In BMDM cells, the blot using antibody ab122624 exhibited a very faint band for cells treated with 10 ng/ml LPS, while for both Acod1 blots band densities peaked for cells treated with 100 ng/ml; fair band densities were visible for cells treated with 5,000 ng/ml LPS. For RAW-264.7 cells, a band corresponding to Acod1 protein appeared only upon treatment with 5,000 ng/ml LPS.

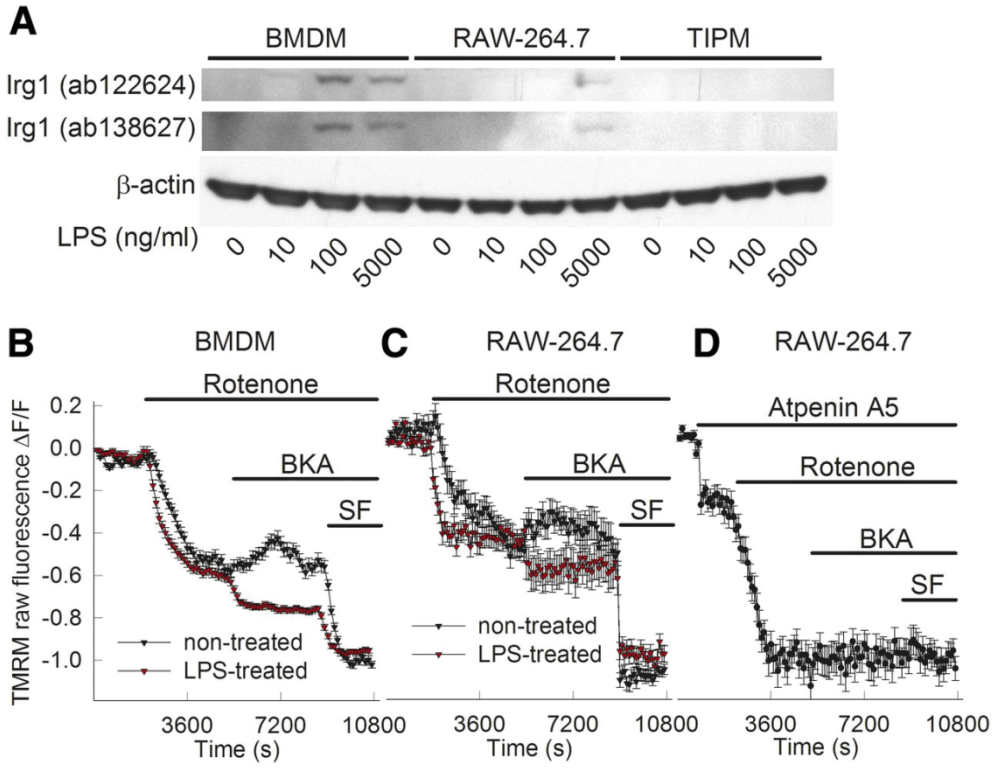

Figure 7. LPS-induced Acod1 (Irg1) expression in macrophages, and abolition of in situ matrix SLP. A: *Scanned Western blot images of BMDM, RAW-264.7 and TIPM cells, challenged by different concentrations of LPS (0, 10, 100 and 5,000 ng/ml) for 12 h. Two different antibodies were raised against different epitopes of the Acod1 protein; equal loading of the wells was verified by β-actin. LPS induces Acod1 expression in BMDM and RAW-264.7 cells at specific LPS concentrations, but not in TIPM cells.* ***B***, ***C:*** *Effect of BKA on the rotenone-evoked depolarization of ΔΨm in cultured BMDM (**B**) and RAW-264.7 (**C**) cells (nontreated, black triangles vs. LPS-treated, red triangles). ΔΨm was followed by potentiometric probe, TMRM. BKA, 20 μM; rotenone, 5 μM. At the end of each experiment, 5 μM SF 6847 was added to achieve complete depolarization. Results are from an average of ~170 cells (**B**) or ~30 cells (**C**). Error bars = SEM. Experiments are representative of 4 independent experiments, each evaluating ~300 BMDM and ~120 RAW-264.7 cells [nontreated vs. LPS-treated (5 μg/ml for 12 h) in 4 individual chambered cover glasses (Lab-Tek)].* ***D:*** *Effect of coinhibition of complex I by 5 μM rotenone and complex II by 1 μM atpenin A5, followed by addition of BKA (20 μM) and SF 6847 (5 μM) in RAW-264.7 cells on TMRM fluorescence.*

Based on Western blotting results, we decided to investigate the effect of LPS at 5,000 ng/ml for 12 hours on matrix SLP in BMDM and RAW-264.7 cells. As shown in Figure 7B and 7C for BMDM and RAW-264.7 cells, respectively, the effect of the cell-permeable inhibitor of the adenine nucleotide translocase, bongkrekic acid (BKA, 20 μM) was recorded. Reflecting ΔΨm of *in situ* mitochondria TMRM fluorescence was used in the presence of rotenone (5 μM). Rotenon is the inhibitor of complex I in the electron transport chain, so it mimics the situation of impaired respiratory chain. Cultures were bathed in an extracellular-like buffer, supplemented with 15 mM glucose as the sole substrate, and TMRM fluorescence was recorded as detailed under "Methods". TMRM is a lipophilic cation accumulated by mitochondria in proportion to ΔΨm. Upon accumulation of the dye it exhibits a red shift in its absorption and fluorescence emission spectrum. The fluorescence intensity is quenched when the dye is accumulated by mitochondria. Addition of the uncoupler SF 6847 (5 μM) at the end of each experiment caused the collapse of ΔΨm. This data was used for the normalization of the TMRM signal of all traces. As it has been previously addressed by our group elsewhere (Chinopoulos et al., 2010; Chinopoulos, 2011a,b; Kiss et al., 2013) the immediate effect of the ANT inhibitor BKA on TMRM fluorescence of rotenone-treated cells "betrays" the directionality of the translocase at the time of the inhibition. The directionality of traces following BKA addition allows us to make conclusion about the presence or absence of matrix SLP mediated by succinate-CoA ligase. BKA-induced repolarization during respiratory chain inhibition implies that succinate-CoA ligase was operating towards ATP (or GTP) formation; by the same token, BKA-induced depolarization during respiratory chain inhibition implies that succinate-CoA ligase was operating towards ATP (or GTP) consumption. As shown in Figure 7B and 7C for BMDM and RAW-264.7 cells, respectively, in nontreated cells (black triangles), BKA caused an increase in TMRM fluorescence, indicating a repolarization. However, in LPS-treated cells (red triangles), BKA caused a depolarization.

From these experiments, we suspected that treatment with LPS induced *Acod1* in BMDM and RAW-264.7 cells causing an increase in itaconate production that abolished matrix SLP.

Itaconate is a weak competitive inhibitor of complex II or succinate dehydrogenase leading to a build-up of succinate, which shifts succinate-CoA ligase

equilibrium towards ATP (or GTP) utilization thus thwarting SLP. We therefore, investigated the effect of the known SDH inhibitor atpenin A5 on rotenone-treated macrophage cells (Figure 7D). As expected, the concomitant inhibition of complex I by rotenone and complex II by atpenin A5 led to a complete collapse of $\Delta\Psi m$, and therefore BKA and SF 6847 exhibited no further loss of TMRM fluorescence; under these bioenergetic circumstances the ANT is completely reversed (Chinopoulos et al., 2010; Chinopoulos, 2011a,b; Kiss et al., 2013) and matrix SLP cannot be addressed.

5.2. The effect of transfecting cells with siRNA directed against *Acod1* on matrix SLP during treatment with LPS

Small (or short) interfering RNA (siRNA) is the most commonly used RNA interference tool for inducing short-term silencing of protein coding genes. The control strategy used for siRNA is the scrambled siRNA that has the same nucleotide composition, but not the same sequence, as the test siRNA.

To verify that LPS treatment impaired matrix SLP by means of itaconate produced by Acod1, we performed silencing experiments directed against *Acod1* expression with siRNA. For these experiments we used RAW-264.7 cells, which typically exhibit high transfection efficiencies (Degrandi et al., 2009), as opposed to primary cells such as BMDMs. Indeed, as shown in Figure 8A, fluorescein-conjugated siRNA or scrambled siRNA decorated >90% of RAW-264.7 cells.

The effect of siRNA and scrambled siRNA transfecting RAW-264.7 cells on *Acod1* expression level as a function of LPS treatment is shown in Figure 8B. RAW-264.7 cells were divided in control, siRNA-transfected and scrambled siRNA transfected tiers, and subdivided in i) no LPS treated *versus* ii) LPS (5 μg/ml) treated, as indicated in the Figure 8B. *Acod1* expression was probed by Western blot. Two different antibodies were used, each rose against different epitopes of the Acod1 protein – the same two antibodies as in Figure 7A. Equal loading of the wells was verified by probing for β-actin. As shown in Figure 8B, control RAW-264.7 cells exhibited *Acod1* expression upon LPS treatment, which was abolished by siRNA transfection directed against *Acod1*. Transfection with scrambled siRNA did not result in abolition of *Acod1*

expression. Similarly to Figure 7A, in the scanned blots it is apparent that there is an excellent agreement of results obtained from the two different anti-Acod1 antibodies.

Next we measured the effect of BKA on the rotenon-evoked depolarization of ΔΨm, detected by TMRM, in cultured RAW-264.7 cells. The effects of ANT inhibitor were compared as follows: in Figure 8C LPS-treated and siRNA transfected against *Acod1* (green triangles) *versus* LPS-treated and scrambled siRNA (black triangles); in Figure 8D LPS-treated and null-transfected (red triangles) *versus* nontreated and null-transfected (black triangles). As shown in Figure 8C, RAW-264.7 cells that have been transfected with scrambled siRNA unaffecting *Acod1* expression, exhibited a BKA-induced depolarization (black triangles), due to the treatment by LPS. However, cells that have been transfected with siRNA directed against *Acod1*, exhibited a BKA-induced repolarization (green triangles). In Figure 8D, RAW-264.7 cells that have undergone null-transfection treatment (neither siRNA nor scrambled siRNA) with LPS (red triangles) or without LPS (black triangles) exhibited similar responses as in Figure 7C.

From these experiments we concluded that LPS treatment caused a reversal in ANT activity of *in situ* rotenone-inhibited mitochondria due to activation of *Acod1* expression.

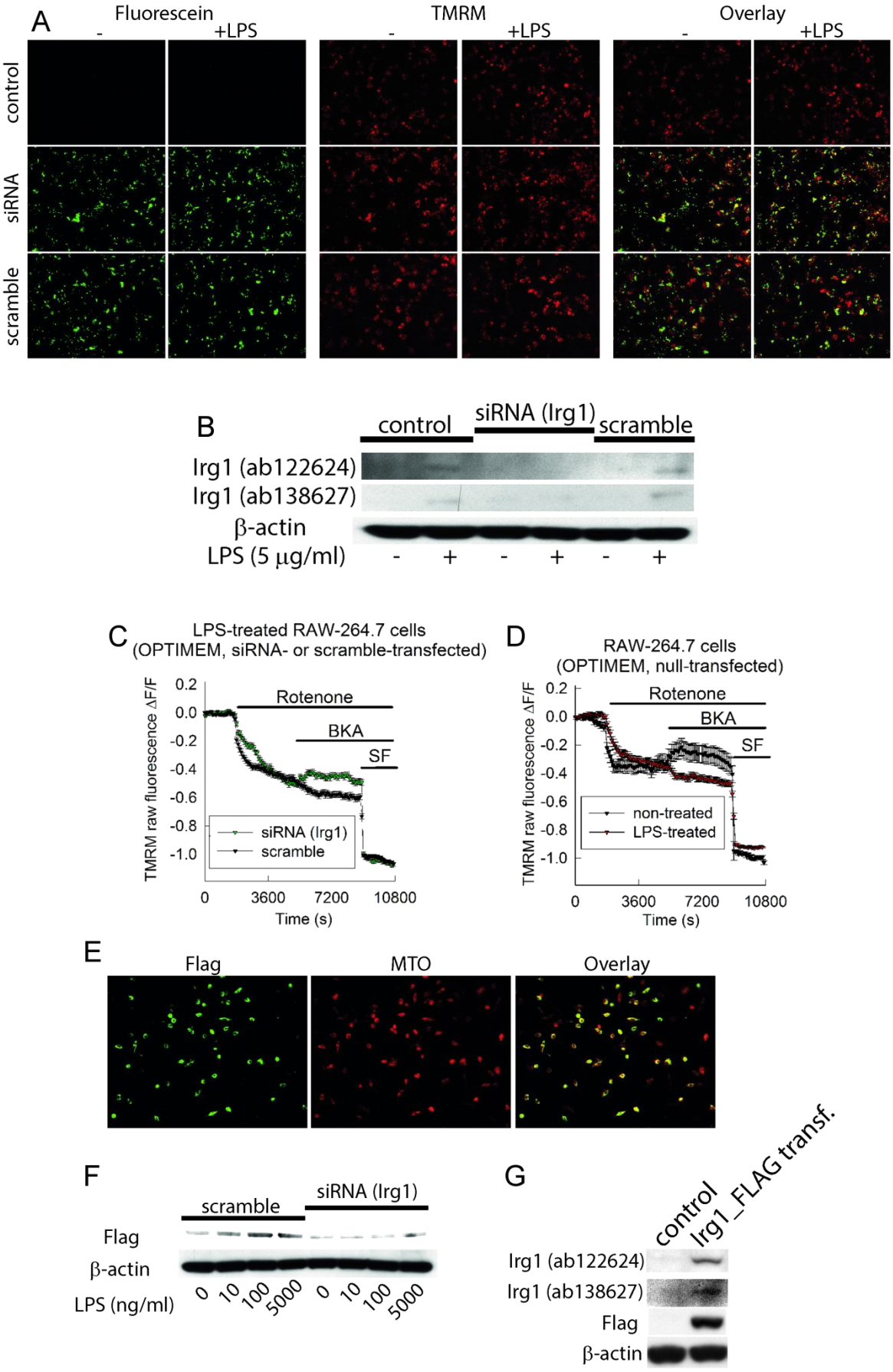
A
Fluorescein
TMRM
Overlay
-
+LPS
control
siRNA
scramble
B
control
siRNA (Irg1)
scramble
Irg1 (ab122624)
Irg1 (ab138627)
β-actin
LPS (5 μg/ml)
C
LPS-treated RAW-264.7 cells
(OPTIMEM, siRNA- or scramble-transfected)
TMRM raw fluorescence ΔF/F
Rotenone
BKA
SF
siRNA (Irg1)
scramble
Time (s)
D
RAW-264.7 cells
(OPTIMEM, null-transfected)
non-treated
LPS-treated
E
Flag
MTO
Overlay
F
scramble
siRNA (Irg1)
Flag
β-actin
LPS (ng/ml)
G
control
Irg1_FLAG transf.
Irg1 (ab122624)
Irg1 (ab138627)
Flag
β-actin

Figure 8. Effect of transfecting cells with siRNA directed against Acod1 (Irg1) on matrix SLP during treatment with LPS. A: *Epifluorescent images of fluorescein (tagging siRNA and scrambled siRNA) and TMRM-loaded (reflecting ΔΨm) RAW-264.7 cells, and their overlays in the presence and absence of LPS (5 μg/ml for 12 h).* ***B:*** *Scanned images of Western blots of RAW-264.7 cells transfected with siRNA directed against Acod1 or scrambled siRNA, further subcategorized in nontreated vs. LPS-treated (5 μg/ml for 12 h), for Acod1 (using 2 different antibodies raised against different epitopes of the Acod1 protein) and β-actin.* ***C:*** *Effect of BKA on the rotenone-evoked depolarization of ΔΨm in cultured RAW-264.7 cells − LPS-treated, scrambled siRNA cotransfected (black triangles) vs. LPS-treated, siRNA directed against Acod1 cotransfected (green triangles).* ***D:*** *Effect of BKA on the rotenone-evoked depolarization of ΔΨm in cultured RAW-264.7 cells − nontreated, null-transfected (black triangles) vs. LPS-treated, null-transfected (red triangles). ΔΨm was followed using the potentiometric probe TMRM. BKA, 20 μM; rotenone, 5 μM. At the end of each experiment, 5 μM SF 6847 was added to achieve complete depolarization. Results shown in panels* ***C*** *and* ***D*** *are from an average of 63-192 cells. Error bars = SEM. The experiments are representative of 4 independent experiments, evaluating 274-690 cells.* ***E:*** *Epifluorescent images of immunocytochemistry decorating FLAG-expressing cells − transfected with the pCMV6-FLAG-Acod1 overexpressing plasmid (left), the mitochondrial network stained with MTO (middle) and the overlays (right). The fluorescence intensity depicted in the image showing the FLAG-expressing cells has been thresholded to expose only the FLAG-expressing cells, due to a minor cross talk of the secondary antibody fluorescence (used for FLAG immunocytochemistry) with the MTO.* ***F:*** *Scanned images of Western blots of RAW-264.7 cells transfected with siRNA directed against Acod1 or scrambled siRNA, cotransfected with the pCMV6-FLAG-Acod1 overexpressing plasmid and further subcategorized in nontreated vs. LPS-treated (dose dependence indicated in the panel) for 12 hours, for the FLAG epitope and β-actin.* ***G:*** *Scanned images of Western blots of COS-7 cells transfected with the pCMV6-FLAG-Acod1 overexpressing plasmid, for Acod1 (using 2 different antibodies raised against different epitopes of the Acod1 protein), the FLAG epitope and β-actin.*

Because the signal-to-noise ratio of the blots using both antibodies directed against Acod1 were admittedly small, which in turn could cast doubt on the efficiency of the siRNA treatment as judged by the Western blot, we attempted to maximize *Acod1* expression in cells where we could more reliably test the affinity of our antibodies, as well as siRNA treatment efficiency. For that, we transfected RAW-264.7 cells with a pCMV6-FLAG-*Acod1* plasmid, known to yield high levels of *Acod1* expression (Michelucci et al., 2013). The plasmid also codes for a FLAG region, for easier identification of the expressed protein by immunotechniques. As shown in Figure 8E, RAW-264.7 cells were identified by MTO labeling of their mitochondrial network and codecorated with antibodies recognizing the FLAG. From the overlay of such images, we deduced that >90% of cells were successfully transfected with the plasmid. By using the same transfection protocols, we evaluated the efficiency of the siRNA *versus* scrambled siRNA treatment in RAW-264.7 cells using Western blot, also treated dose-dependently with LPS. As shown in Figure 8F, RAW-264.7 cells tested positive for FLAG expression, and those that were cotransfected with the scrambled siRNA against *Acod1* exhibited a dose-dependent increase in FLAG expression; this is not surprising, because the CMV promoter (controlling the *Acod1* expression in the pCMV6-FLAG-*Acod1* plasmied) is known to be affected by LPS through TLR (Lee et al., 2004), which is present in the RAW cells. Moreover, cotransfection of RAW cells overexpressing FLAG-*Acod1* with siRNA directed against *Acod1* abolished the dose-dependent increase in FLAG expression by the LPS (right part of Figure 8F).

From these experiments we concluded that the siRNA could effectively diminish the expression of *Acod1* in these cells.

To address the quality of the anti-Acod1 antibodies, we transfected COS-7 cells with the pCMV6-FLAG-*Acod1* plasmid exactly as for the RAW-264.7 cells. In these cells we then probed for Acod1 protein and the FLAG by Western blot. As shown in Figure 8G, only the transfected cells exhibited immunoreactivity for the anti-Acod1 and the anti-FLAG antibodies. Anti-Acod1 ab122624 exhibited a slightly better signal-to-noise ratio as compared to blots shown in Figure 7A and 8B, in line with an expected increased expression of Acod1 protein, but this was not apparent for antibody ab138627.

5.3. The effect of LPS treatment on oxygen consumption and extracellular acidification rates in macrophages

Metabolic changes in macrophages and their functional polarization are intricately connected (Zhu et al., 2015). LPS-induced activation of TLR4 generates numerous downstream effects among which glycolytic and mitochondrial respiration pathways are known to occur (Everts et al., 2012; Través et al., 2012; Tavakoli et al., 2013). Therefore, we examined the dose-dependent effect of LPS treatment in both BMDM and RAW-264.7 cells on oxygen consumption rates and extracellular acidification rates.

Most cells possess the ability to shift dynamically between the two major energy producing pathways, glycolysis and oxidative phosphorylation. Cells take up glucose and oxygen, and process them biologically to generate ATP, while extruding products such as lactate, H^+ and CO_2 into the extracellular environment. In the cytosol glucose is processed to pyruvate, which is during aerobic respiration (or oxidative phosphorylation) converted to CO_2 and water in the mitochondria, or under anaerobic conditions converted to lactate in the cytoplasm. Some cells, as it is the case with tumor cells or LPS-induced macrophages, even under aerobic conditions prefer glycolysis ending with lactate over oxidative phosphorylation. ATP produced during oxidative phosphorylation is 18 folds higher than during glycolysis.

When glycolysis-derived lactate is exported from the cell, protons are also exported. Extracellular acidification rate is thus an indicator of glycolysis, while oxygen consumption rate is an indicator of mitochondrial respiration. Cellular oxygen consumption (respiration) and proton excretion (glycolysis) causes rapid and easily measurable changes in living cells. Seahorse Metabolic Analyzer simultaneously measures OCR and ECAR.

However, it is important to mention, that beside lactate, another potential source of extracellular protons is CO_2, generated during mitochondrial substrate oxidation. CO_2 is hydrated to H_2CO_3, which then dissociates to HCO_3^- and H^+; the contribution of HCO_3^- produced acidification depends on the cell type and substrate, and may vary from 3% to 100% of the total acidification rate (Mookerjee et al., 2015). Therefore, measurements of extracellular acidification rates are bound to be affected by CO_2 production during mitochondrial substrate oxidation. However, as it will be shown

below, increases in ECAR are associated with decreases in OCR, implying that alterations in ECAR are mostly due to changes in glycolytic fluxes, and not due to changes in CO_2 production during mitochondrial substrate oxidation.

BMDM cells (Figure 9B, D, F and H) and RAW-264.7 cells (Figure 9A, C, E and G) were probed for OCR (Figure 9, top panels) and ECAR (Figure 9, bottom panels) under various, sequential metabolic conditions as indicated in the panels, in the presence and absence of glucose, and at different concentrations of LPS (0, 10, 100 and 5000 ng/ml, all for 12 hours). The medium contained 2 mM glutamine – glutamine provides carbon skeleton to the citric acid cycle intermediates. As shown in Figure 9C and 9D, addition of glucose resulted in a robust decrease in the basal level of respiration. This response is typical for macrophage cells upon activation of TLR, switching on aerobic glycolysis in addition to maintaining oxidative phosphorylation (Krawczyk et al., 2010, Rodríguez-Prados et al., 2010) – an effect that is also characteristic for tumor cells (Vander Heiden et al., 2009). Addition of medium instead of glucose (Figure 9A and 9B) did not yield similar changes in OCR as glucose, thus serving as a "vehicle" control. Afterwards, applying oligomycin, the F_o-F_1 ATP synthase inhibitor, further decrease in OCR is visible (Figure 9C, D). It is used to assess oxygen consumption associated to ATP synthesis, and this decrease in OCR is independent from the presence or absence of glucose (Figure 9A, B). Next, 2,4-dinitrophenol (DNP) was added, which is an uncoupler – it uncouples electron transport in the respiratory chain from oxidative phosphorylation. In living cells, DNP acts as a proton ionophore, an agent that can shuttle hydrogen cations (H^+) across the inner mitochondrial membrane. It stimulates oxygen consumption without a concomitant increase in ATP production. In presence of uncoupler oxygen combines with H^+ without the formation of ATP. Uncoupling of the oxidative phosphorylation with DNP resulted in maximal respiration in both RAW-264.7 and BMDM cells (Figure 9C and 9D, respectively); in RAW-264.7 cells, this was unaffected by LPS, at any concentration tested (Figure 9C); on the other hand, the DNP-induced maximal respiration was dose-dependently abolished by LPS in BMDM cells (Figure 9D). Coapplication of antimycin A with rotenone (A+R) inhibiting mitochondrial complex III and I, respectively, completely shuts down the ETC, and as such dramatically suppressed OCR in both cell types.

In parallel with OCR, ECAR changes are also detected. The increases in ECAR (Figure 9G and 9H) upon the injection of glucose implied a shift in the metabolism from mitochondria to glycolysis. In the absence of glucose, when only medium was applied, no changes in basal ECAR were observed (Figure 9E and 9F). Without additional glucose ECAR reflects CO_2 production during mitochondrial substrate oxidation. This ECAR level is decreased by the F_o-F_1 ATP synthase inhibitor, oligomycin – parallel with drop in synthesised ATP, the TCA cycle intensity and also the production of CO_2 during mitochondrial substrate oxidation is reduced. The uncoupler DNP, on the contrary, increases ECAR level – oxygen is reduced by reducing equivalents originating from TCA cycle, which contributes to CO_2-produced acidification. Coapplication of complex III and I inhibitors decrease the ECAR reflecting that together with inhibited ETC the TCA cycle is also reduced. It is apparent that uncoupling of BMDM cells by DNP led to statistically significant changes in ECAR, which were dose-dependently abolished by LPS (Figure 9F). This cannot be said for RAW-264.7 cells (Figure 9E) – there are no dose-dependent changes upon DNP application. Along the same lines, in cells with additional glucose LPS had a dose-dependent effect on increasing ECAR in BMDM (Figure 9G) but not RAW-264.7 cells (Figure 9H). In cells where glucose is present ECAR reflects changes in glycolytic flux, therefore addition of inhibitors of ETC have no significant effect. What is also apparent from the above results is that RAW-264.7 cells are more reliant on glycolysis for energy production than BMDM cells (compare OCR and ECAR basal rates between the cell types); this is probably because RAW-264.7 cells already exhibit maximal upregulation in glycolytic enzymes, as opposed to BMDM cells where an LPS effect in upregulating glycolysis further, in conjunction with inhibiting mitochondrial oxidation, can be demonstrated.

Mindful that no significant difference was observed in mitochondrial and glycolytic parameters between LPS-stimulated and non-stimulated RAW-264.7 cells, and that in the same cells LPS abolished SLP, we concluded that the effect of LPS on SLP was exclusively attributed to induction of *Acod1* yielding itaconate, and was not due to circumstantial bioenergetic effects involving glycolysis and/or oxidative phosphorylation.

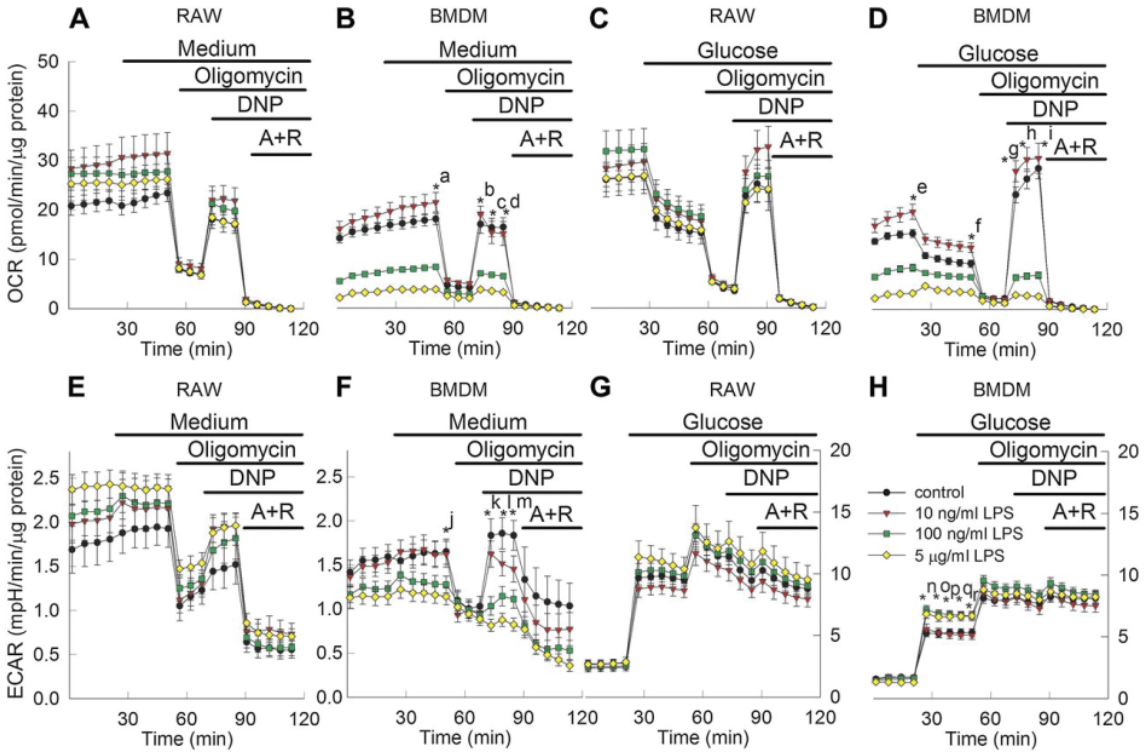

Figure 9. Effect of LPS on BMDM and RAW-264.7 cells on OCR and ECAR in the presence or absence of glucose, upon addition of various metabolic inhibitors. *OCR and ECAR were determined in a microplate format respirometry/pH assay using a Seahorse XF96 Analyzer. Glucose, 10 mM; oligomycin, 2 µM; DNP, 100 µM; antimycin, 1 µM; rotenone, 1 µM. The medium contained 2 mM glutamine. Data are from 3 independent cell culture preparations, n=10-12 wells, each containing ~25,000-50,000 RAW-264.7 cells or n=12-25 wells, each containing ~50,000 BMDM cells. Panels* ***A-D*** *are aligned in the y axis (OCR). Whenever error bars are not visible, it is because they are smaller than the symbol size. Data are presented as mean ± SEM; significant differences between groups of data were evaluated by 1-way ANOVA followed by Dunnett's post hoc analysis (control = no LPS treatment), with P < 0.05 considered as significant. *a, *b, *c, *d, *h, *i, *k, *l, *m, *n, *o, *p, *q, *r: P < 0.001, compared to 100 ng/ml, 5 µg/ml LPS; *e, *f, *g: P < 0.001, compared to 10 ng/ml, 100 ng/ml, 5 µg/ml LPS; *j: P = 0.006, compared to 5 µg/ml LPS. All other data comparisons were not statistically significant. LPS concentrations indicated in the panel* ***H****.*

5.4. Categorization of respiratory substrates used for isolated mitochondria

To elaborate further on the exact mechanism(s) of itaconate inhibiting SLP, we investigated the dose-dependent effect of exogenously added itaconate to isolated mitochondria, under defined metabolic conditions. In the experiments using isolated mitochondria it is critical to use adequate substrate combinations to maintain mitochondrial respiration.

Substrates could be categorized to those that participate directly in citric acid cycle, those that participate indirectly in tricarboxylic acid cycle, and those not at all participating. Substrates participating directly in the citric acid cycle are: α-ketoglutarate, succinate, fumarate, malate; those involved indirectly are: pyruvate, aspartate, glutamate; and those having no share are: β-hydroxybutyrate, acetoacetate. Another possible categorization of substrates is to those that support SLP, or not.

Glutamate and α-ketoglutarate are the two substrates that support SLP to the greatest extent (Figure 1). Glutamate can enter the citric acid cycle through the reaction catalized by glutamate dehydrogenase, which coverts glutamate to α-ketoglutarate. Malate alone has no effect, but it assists in the entry into mitochondria of other substrates including glutamate and α-ketoglutarate, thus indirectly supporting SLP. Pyruvate and aspartate, alone or in combination, support substrate-level phosphorylation very weakly. Acetoacetate (AcAc) and β-hydroxybutyrate alone are also without a direct effect on SLP; however, AcAc leads to NAD^+ regeneration through the reaction catalyzed by β-hydroxybutyrate dehydrogenase, that boosts SLP supported by glutamate (or α-ketoglutarate) yielding succinyl-CoA through the α-ketoglutarate dehydrogenase complex; β-hydroxybutyrate would not support SLP even in presence of glutamate (or α-ketoglutarate), because it competes for NAD^+ with KGDHC. Succinate and fumarate disfavours SLP. When succinate is in excess, it is not only converted to fumarate, but in equilibrium with succinyl-CoA, and as such keeps the reversible SUCL reaction towards succinyl-CoA formation and ATP depletion. Similarly, accumulated fumarate is in equilibrium with succinate, and by this way, shifts the TCA cycle in reverse, that is, succinyl-CoA plus ADP plus P_i formation.

In synchrony with our aim to study the inhibitory effect of itaconic acid on SLP, substrates supporting SLP were chosen in the following experiments.

5.5. The dose-dependent effect of itaconate on ANT directionality in rotenone-treated isolated mitochondria

Similarly to *in situ* mitochondria, SLP can be investigated in intact isolated mitochondria with an inhibited respiratory chain using a "biosensor test" employed successfully by our group (Chinopoulos et al., 2010). In the case of isolated mitochondria the effect of the adenine nucleotide translocase inhibitor carboxyatractyloside could be investigated on safranine O fluorescence reflecting ΔΨm. Safranine O is a lipophilic cationic dye. Its potential-dependent distribution between two sides of the inner mitochondrial membrane (stacked to anions on the matrix side) undergoes optical shift. Since one molecule of ATP^{4-} is exchanged for one molecule of ADP^{3-} (both nucleotides being Mg^{2+}-free and deprotonated) by the ANT, the exchange is electrogenic (Klingenberg, 2008). Therefore, abolition of the ANT by cATR when it functions in the forward mode (translocating ADP^{3-} into and ATP^{4-} out of the matrix) leads to an increase in ΔΨm (shift toward more negative values), whereas the same condition leads to a loss of ΔΨm (shift toward less negative values) when the ANT is working in reverse mode (translocating ATP^{4-} into and ADP^{3-} out of the matrix). In the presence of sufficient SLP, the ANT is expected to operate in the forward mode even when the electron transport chain is inhibited by rotenone. By the same token, in the absence of sufficient SLP, the ANT is expected to operate in the reverse mode in the presence of rotenone.

In Figure 10A, the effect of itaconate (always present in the media before addition of mitochondria, b: 0.5 mM, c: 1 mM, d: 2 mM, e: 5 mM) on the ANT operation is shown as compared to control a, for mitochondria supported by glutamate (5 mM) and malate (5 mM). The sequence of additions, identical for each panel, was the following: mitochondria were allowed to polarize, followed by the addition of 2 mM ADP, which depolarized mitochondria to a variable level depending on the substrate combinations (Berg et al., 2002; Chinopoulos et al., 2009), indicated in the panels. After 100 sec during which a substantial amount of ADP has been converted to ATP, complex I was inhibited by rotenone (1 μM) which "clamped" ΔΨm at approximately –100 mV, again depending on the substrate combinations. After an additional 150 s, cATR (2 μM) was added to block ANT. At the end of each experiment the uncoupler SF 6847 (1 μM) was added in order to completely depolarize mitochondria; this would assist in the

calibration of the safranine O signal. It is evident that the forward operation of ANT observed in the control tends to be inhibited, even reversed in the presence of increasing concentration of itaconate, indicating an inhibitory action of this compound on SLP.

Similar conclusion is drawn from experiments with other substrate combination. In Figure 10B, the effect of itaconate (b: 0.25 mM, c: 0.375 mM, d: 0.5 mM, e: 1 mM) *versus* control is shown for mitochondria supported by α-ketoglutarate (5 mM) and malate (5 mM). It is evident that with increasing concentrations of itaconate, cATR resulted in depolarization, compared to repolarization observed in the absence of this compound. Similar experiments with itaconate (b: 0.5 mM, c: 2 mM) are shown in Figure 10C for mitochondria supported by glutamate (5 mM) plus malate (5 mM) plus acetoacetate (AcAc, 0.4 mM). The latter result is consistent with the fact that AcAc increases [NAD^+] in the mitochondrial matrix, thus boosting succinyl-CoA production by KGDHC (Kiss et al., 2013; Kiss et al., 2014). In Figure 10D, the effect of mesaconate (always present in the media before addition of mitochondria, b: 5 mM, c: 10 mM) *versus* control a is shown, obtained in the presence of glutamate (5 mM) and malate (5 mM). Consistent with the findings by Adler *et al.* (Adler et al., 1957), and Wang *et al*. (Wang et al., 1961), mesaconate was much less potent than itaconate in exerting an impact on SLP.

From the above results, we concluded that itaconate abolished SLP in isolated mitochondria in which the respiratory chain was inhibited.

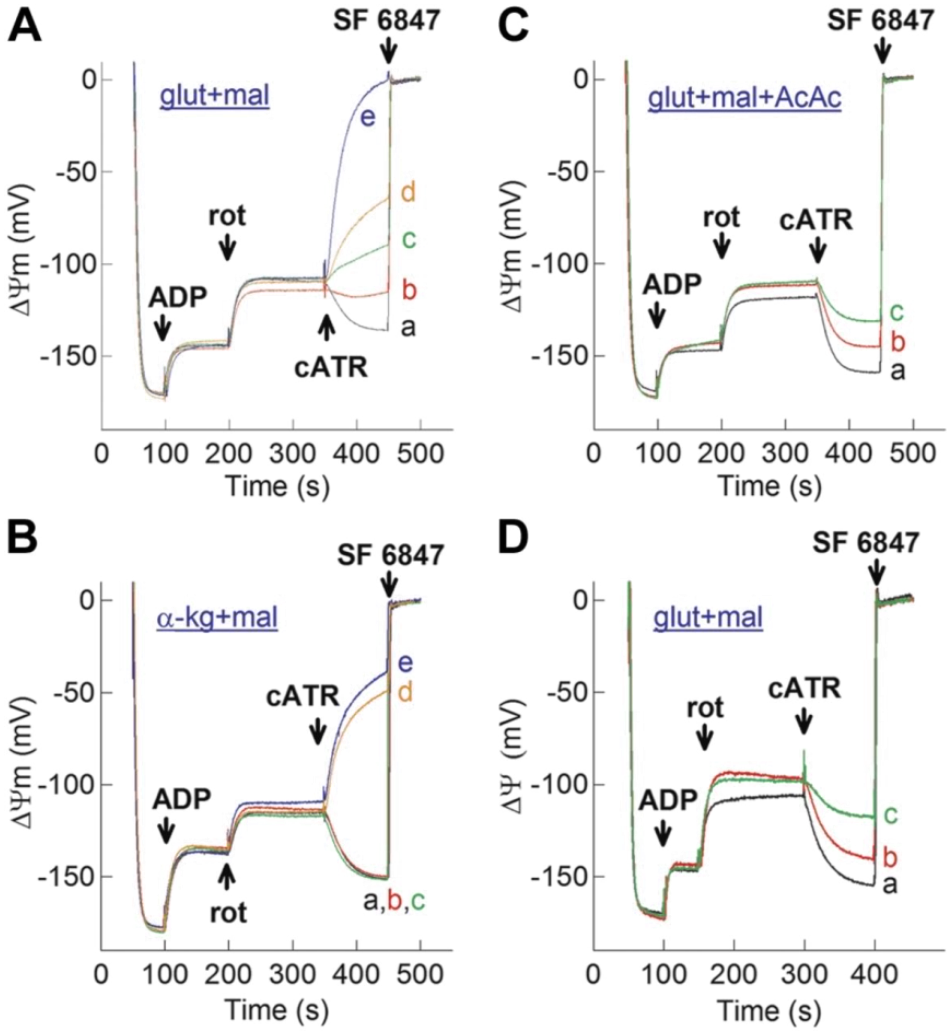

Figure 10. Reconstructed time courses of safranine O signal calibrated to ΔΨm in isolated mouse liver mitochondria supported by various substrates as indicated in the panels. *The effect of cATR (2 μM) on ΔΨm of mitochondria treated with rotenone (rot, 1 μM, where indicated) in the presence or absence of itaconate (**A**, **B**, **C**) or mesaconate (**D**) is shown. ADP (2 mM) was added where indicated. Itaconate concentrations (present prior to addition of mitochondria) are as follows, in mM: a: 0, b: 0.5, c: 1, d: 2, e: 5 (**A**); a: 0, b: 0.25, c: 0.375, d: 0.5, e: 1 (**B**); a: 0, b: 0.5, c: 2 (**C**). Mesaconate concentrations (present prior to addition of mitochondria) are as follows, in mM: a: 0, b: 5, c: 10 (**D**). At the end of each experiment, 1 μM SF 6847 was added to achieve complete depolarization.*

5.6. The effect of malonate on ANT directionality in rotenone-treated isolated mitochondria

As it is mentioned earlier, itaconate is a mild inhibitor of SDH (also known as complex II). SDH is the only membrane-bound enzyme in the citric acid cycle. It contains FAD as coenzyme, which is reduced to $FADH_2$, and then further transducing reducing equivalents to the electron transport chain. Malonate is a classical competitive inhibitor of SDH. This analog of succinate is normally not present in cells. Addition of malonate to mitochondria blocks the activity of the citric acid cycle.

We investigated if the effect of itaconate was due to a mild inhibition of SDH leading to accumulation of succinate thus shifting the succinate-CoA ligase equilibrium towards ATP (or GTP) consumption, or due to consumption of ATP (or GTP) for itaconyl-CoA formation, or both. The effects of itaconate were compared to that of malonate. As malonate is not metabolized by succinate-CoA ligase, it was necessary to titrate the concentrations of itaconate and malonate so that they exhibit SDH inhibition to similar extent. Itaconate and malonate were always present in the medium prior addition of mitochondria. The effect of itaconate *versus* malonate on OCRs was examined on state 2 and state 3 respiration (induced by 2 mM ADP) in mitochondria supported by 5 mM succinate in the presence of 1 μM rotenone.

State 2 and 3 refer to certain mitochondrial respiratory conditions. When the medium contains only isolated mitochondria and added substrate(s), it is called, state 2 respiration. During this state respiration is low due to lack of ADP (only some intrinsic substrates and ADP is present). Following the addition of ADP to the medium, the respiration changes to state 3. Under experimental conditions usually a limited amount of ADP is added, allowing rapid respiration.

When oxygen is available cells respire to generate ATP. Under experimental conditions oxygen used from the medium could be detected, what we call oxygen consumption rate. In normally respiring mitochondria OCR is high, while it is the opposite in respiratory chain inhibited mitochondria. As it is shown on Figure 11A and 11B the effect of itaconate and malonate, respectively, on OCRs are expressed. In state 2, when only substrate (in this case, succinate) and mitochondria are pesent, as well as, SDH inhibitors, itaconate or malonate, there are no detectable differences in OCRs – without ADP there is no respiration. In state 3, when respiration is induced by ADP,

SDH inhibitors in concentration dependent manner decreased OCRs (Figure 11A and 11B). It is also evident that 1 mM itaconate conferred a similar decrease in oxygen consumption as 125 μM malonate; likewise, 5 mM itaconate conferred a similar decrease in oxygen consumption as 500 μM malonate. Therefore, we deduced that itaconate was approximately ~8 to 10 times less potent than malonate in inhibiting succinate-supported mitochondrial respiration. However, as shown in Figure 11C, malonate, in concentrations exhibiting similar effect on O_2 consumption to those by itaconate, conferred greater ADP-induced depolarizations than itaconate in mitochondria supported by 5 mM succinate in the presence of 1 μM rotenone. The effect of malonate (added prior to mitochondria, supported by glutamate and malate) on cATR-induced changes in $\Delta\Psi m$ in the presence of rotenone is shown in Figure 11D (b: 0.0625 mM, c: 0.125 mM, d: 0.25 mM, e: 0.5 mM, f: 5 mM; malonate *versus* control a). It is evident that malonate conferred cATR-induced depolarizations at concentrations in which they inhibit succinate-supported respiration to the same extent as itaconate. However, at the very same concentrations, malonate conferred greater ADP-induced depolarizations than itaconate in mitochondria respiring on succinate in the presence of rotenone.

We could not demonstrate itaconate-mediated respiration as shown by Adler *et al.* (Adler et al., 1957) and Wang *et al.* (Wang et al., 1961) (data not shown). However, in their experiments mitochondria were incubated for several hours with itaconate, which might lead to sufficient conversion to a suitable product further oxidized by SDH.

From the above results we concluded that the abolition of SLP by itaconate cannot be exclusively attributed to favouring itaconyl-CoA formation requiring ATP (or GTP) for the thioesterification, or to inhibition of complex II leading to a build-up of succinate which shifts succinate-CoA ligase equilibrium towards ATP (or GTP) utilization.

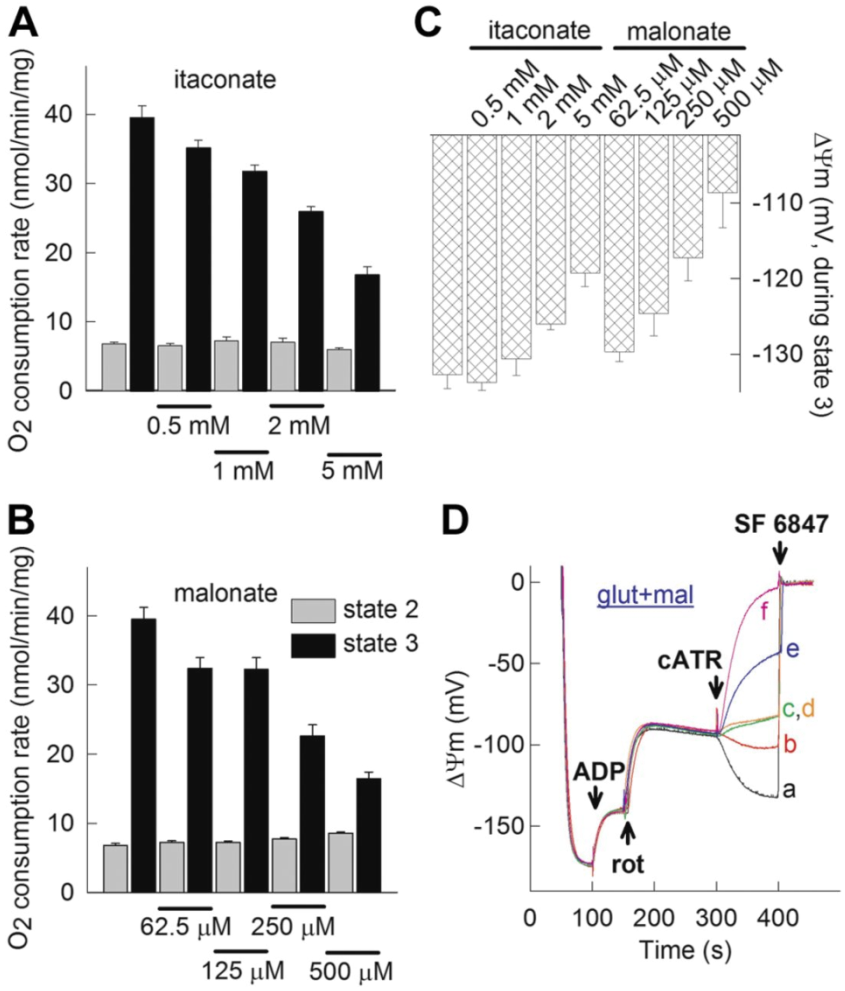

Figure 11. Effects of itaconate and malonate on SDH. *Bar graphs of the effect of itaconate (**A**) and malonate (**B**) on OCRs expressed as nmol/min/mg protein (state 2, grey bars; state 3 induced by 2 mM ADP, black bars), in isolated mitochondria respiring on succinate (5 mM) in the presence of rotenone (1 µM).* ***C:*** *Bar graphs of the effect of itaconate and malonate on ΔΨm expressed in mV during state 3 (induced by 2 mM ADP), in isolated mitochondria respiring on succinate (5 mM) in the presence of rotenone (1 µM). Concentrations of itaconate and malonate are indicated in the panel.* ***D:*** *Reconstructed time courses of safranine O signal calibrated to ΔΨm in isolated mouse liver mitochondria supported by glutamate (5 mM) and malate (5 mM). The effect of cATR (2 µM) on ΔΨm of mitochondria treated with rotenone (rot, 1 µM, where indicated) in the presence of malonate is shown. ADP (2 mM) was added where indicated. Malonate concentrations (present prior to addition of mitochondria) are as follows, in mM: a: 0, b: 0.0625, c: 0.125, d: 0.25, e: 0.5, f: 5. At the end of each experiment, 1 µM SF 6847 was added to achieve complete depolarization.*

5.7. The effect of the succinate-CoA ligase inhibitor KM4549SC on ANT directionality in rotenone-treated isolated mitochondria

In the absence of oxygen or when the electron transport chain is impaired, SLP is the only source of high-energy phosphates produced in mitochondria. In the experiments presented in this thesis the key enzyme of SLP, succinate-CoA ligase was manipulated in means of substrates supporting its operation or not, but never by targeting the enzyme itself. At this point we considered to check whether inhibition of succinate-CoA ligase could have an impact on the effect of cATR-induced alterations in ΔΨm in respiration-impaired mitochondria. To elucidate this, we used KM4549SC (LY266500), an inhibitor of succinate-CoA ligase (Hunger-Glaser et al., 1999). As shown in Figure 12, ΔΨm was measured by safranine O fluorescence in mouse liver mitochondria respiring on different substrates. The sequence of additions is identical for each panel, and it is the same as described in section "The dose-dependent effect of itaconate on ANT directionality in rotenon-treated isolated mitochondria". It is evident that KM4549SC reverted the cATR-induced repolarizations (black traces, control) to depolarizations (red and green traces) in a concentration depending manner as shown in Figure 12A, B, D and F. In Figure 12C and E the inhibitor did not lead to a cATR-induced depolarization due to the presence of AcAc, which increases [NAD^+] in the mitochondrial matrix, supporting succinyl-CoA production by KGDHC (Kiss et al., 2013; Kiss et al., 2014). In the experiments shown in Figure 12F, AcAc was also present, but glutamate or α-ketoglutarate were absent. For detailed effects of substrates on SLP, see the section "Categorization of respiratory substrates used for isolated mitochondria".

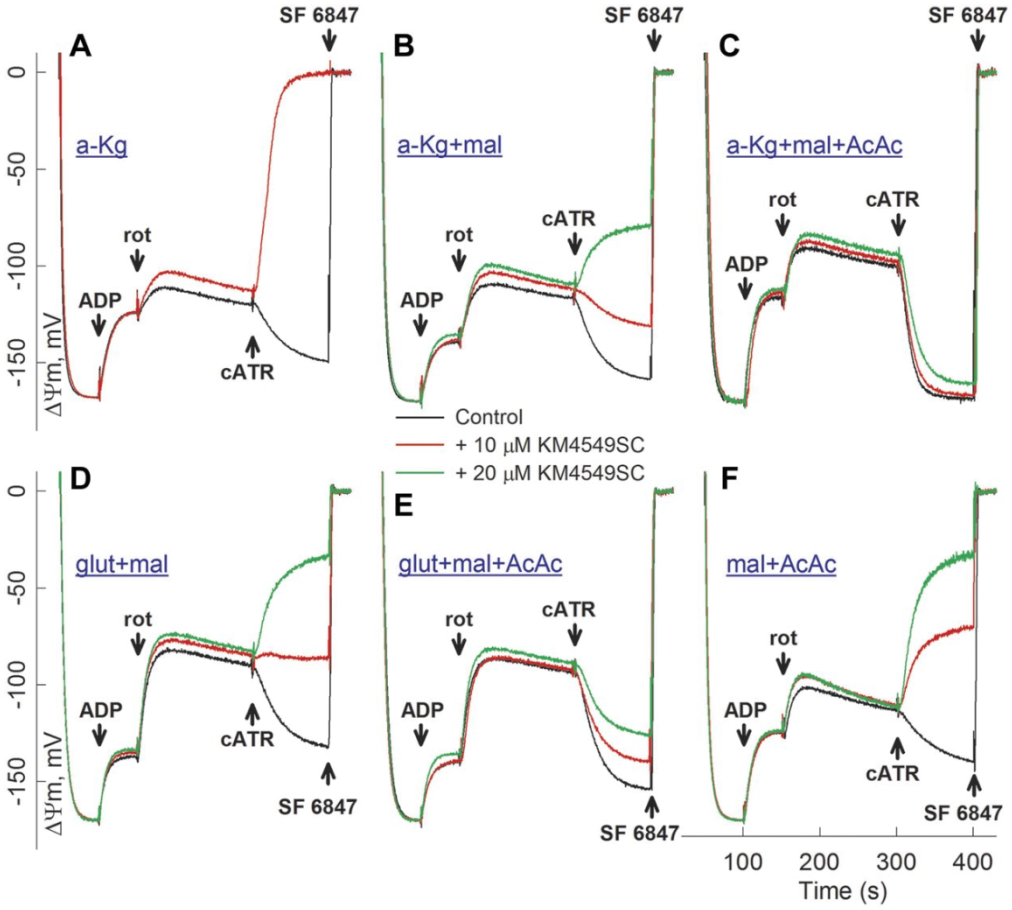

Figure 12. Reconstructed time courses of safranine O signal calibrated to ΔΨm in isolated mouse liver mitochondria supported by various substrates as indicated in the panels. *The effect of cATR (2 μM) on ΔΨm treated with rotenone (rot, 1 μM) in the absence or presence of KM4549SC in 10 μM (red traces) or 20 μM (green traces) concentrations is shown. ADP (2 mM) was added where indicated. Control traces are shown in black. At the end of each experiment, 1 μM SF 6847 was added to achieve complete depolarization. Each panel shares the same x axis as shown in panel* ***F****.*

According to the data from the literature, KM4549SC is a specific inhibitor of mitochondrial succinate-CoA ligase, and an irreversible, or a very tightly binding inhibitor of SUCL phosphorylation (Hunger-Glaser et al., 1999). To exclude an effect of KM4549SC elevating succinate concentration (thus inhibiting substrate-level phosphorylation) by inhibiting SDH, we determined SDH activity in the presence and absence of this chemical. As it is shown in Figure 13, KM4549SC had no effect on SDH activity.

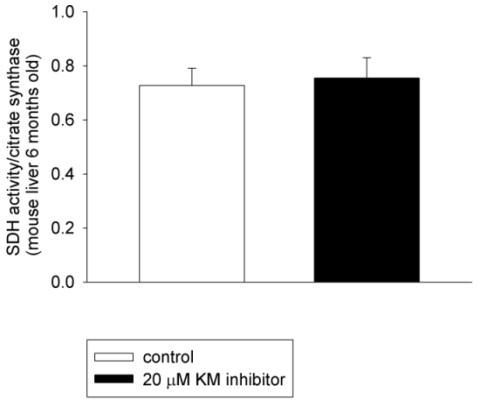

Figure 13. Bar graphs of SDH activity from mice liver mitochondria.

It is concluded from the above results that inhibition of succinate-CoA ligase led to cATR-induced depolarization in mitochondria with an inhibited respiratory chain. This lends further support to the hypothesis that ATP (or GTP) provision by this reaction is critical for maintaining the forward mode of the ANT as suggested in respiration-impaired mitochondria (Chinopoulos et al., 2010; Kiss et al., 2013; Kiss et al., 2014), and therefore underlies the impact of itaconate in abolishing this mechanism.

6. DISCUSSIONS

This work provides a novel and interesting role for the itaconic acid generated by activated macrophages. Previously others showed that itaconate has antimicrobial activity. The concept of itaconate as an antimicrobial compound was supported by the findings that many pathogens require itaconate utilization for pathogenicity. However, the effect of itaconate on the metabolism of the host are largely unexplored, our findings provides novel exciting insights in this topic. Based on our results, we propose that macrophages, and similar lineage cells, loose SLP, caused by itaconate, and this is necessary for them to mount an immune response.

In our earlier works SLP was given an important role in the absence of oxygen or when the electron transport chain is impaired. We investigated in details the mechanisms of SLP (Chinopoulos et al., 2009; Chinopoulos, 2011a; Kiss et al., 2013; Kiss et al., 2014). Step by step the different aspects of SLP were revealed. First of all it became clear that during respiratory arrest, when F_o-F_1 ATP synthase reverses ANT is still able to operate in forward mode (exporting ATP out of matrix, and importing ADP for exchange). This is only possible if SLP is in operation. As it is known, in mitochondrial matrix SLP is addressed to the reversible reaction catalyzed by SUCL. This reaction is part of the citric acid cycle, which favors the conversion of succinyl-CoA and ADP (or GDP) to CoASH, succinate and ATP (or GTP). SUCL does not require oxygen to produce ATP, and it is even activated during hypoxia (Phillips et al., 2009). It is obvious that under normal physiological conditions provision of ATP by SLP works in parallel with oxidative phosphorylation (Johnson et al., 1998b), still during impaired respiratory chain the functionality and importance of SLP comes into foreground. For uninterrupted operation of SUCL, the enzyme requires provision of its substrate, *i.e.* succinyl-CoA. From textbooks it is known that provision of succinyl-CoA through KGDHC is much higher than that originating from propionyl-CoA metabolism (Stryer, 1995). The next big breakthrough of our group was the discovery that supply of succinyl-CoA by KGDHC plays an important role in operation of SLP. The α-ketoglutarate dehydrogenase complex is an enzyme consisting of multiple copies of three subunits: α-ketoglutarate dehydrogenase (KGDH or E1k, EC 1.2.4.2), dihydrolipoyl succinyltransferase (E2k or DLST, EC 2.3.1.61), and dihydrolipoyl dehydrogenase (DLD or E3, EC 1.8.1.4). It participates in the TCA cycle, where it

irreversibly catalyzes the conversion of α-ketoglutarate, CoASH and NAD^+ to succinyl-CoA, NADH and CO_2. In the experiments two types of transgenic mouse strains were generated, one lacked the DLST subunit, and the other lacked the DLD subunit (Kiss et al., 2013). Disruption of both alleles of either gene resulted in perigastrulation lethality; heterozygote mice exhibited no apparent behavioral phenotypes. The findings demonstrated that the decreased provision of succinyl-CoA diminishes matrix SLP, resulting in impaired mitochondrial ATP output and consumption of cytosolic ATP by respiration-impaired mitochondria. Transgenic mice with a deficiency of either dihydrolipoyl succinyltransferase (DLST) or dihydrolipoyl dehydrogenase (DLD) exhibited a 20-48% decrease in KGDHC activity. Taking into account the reaction catalyzed by KGDHC, the question arises about the source of NAD^+ when the ETC is dysfunctional. It is common knowledge that NADH generated in the citric acid cycle is oxidized by complex I, resupplying NAD^+ to the cycle. In the absence of oxygen or when complexes are not functional, an excess of NADH in the matrix is expected. Yet, our previous reports showed that without NADH oxidation by complex I of the respiratory chain, SLP is operational and supported by succinyl-CoA (Chinopoulos et al., 2010; Kiss et al., 2013), implying KGDHC activity. The step by step exploration of SLP led us to the study where we found that during anoxia or pharmacological blockade of complex I, mitochondrial diaphorases oxidized matrix NADH supplying NAD^+ to KGDHC, which in turn yields succinyl-CoA, thus supporting SLP (Kiss et al., 2014).

From different aspects the relevance and importance of SLP during respiratory arrest was proven. Mitochondria are capable of keeping their integrity and $\Delta\Psi m$ under suboptimal level thanks to operation of SLP. Functional SLP means survival of the cell, of the host. And yet, abolishing SLP also could mean a survival for the host. It is like two sides of the same coin, but being equally favourable – one mechanism, *i.e.* SLP, which has two outcomes (functional or abolished), and still provides beneficial effect to the host. Focusing on our experiments, one side of the coin is when we proved that SLP is substantial during respiratory arrest, and it is important for the survival of the host; the other side of the coin is the realization that under certain conditions abolition of SLP could be favourable for the host – through this study this "other side of the coin" is discussed.

In the present thesis it is reported that by inducing *Acod1* in BMDM and RAW-264.7 cells with LPS, which is expected to lead to an increase in endogenous itaconate production (Strelko et al., 2011; Michelucci et al., 2013), *in situ* matrix SLP is also abolished. This is in accordance with recent findings showing that LPS increased succinate levels (Tannahill et al., 2013; Mills ans O'Neill, 2014). In the latter studies this was attributed to i) increased glutamine uptake in LPS-activated macrophages and subsequent anaplerosis of α-ketoglutarate into the citric acid cycle leading to elevated succinate production, and ii) LPS-induced up-regulation of the GABA shunt, a pathway that eventually also led to increased levels of succinate. However, the possibility of LPS inducing *Acod1* resulting in itaconate production, which in turn subsequently inhibits SDH and favors itaconyl-CoA production leading to a CoA trap abolishing SLP, has been overlooked. Our findings imply that the latter scenarios are also likely to unfold; moreover, they are not at odds with the possibilities of increased glutamine uptake leading to elevated succinate production by anaplerosis, or the up-regulation of the GABA shunt.

The likelihood of the mechanism operating in cells of macrophage lineage proposed hereby is supported by our results on exogenously added itaconate to isolated mitochondria; there, in isolated mouse liver mitochondria with an inhibited respiratory chain, itaconate dose-dependently reverted the cATR-induced repolarization to a depolarization, thus implying an abolition of SLP. Because this effect could be reproduced by malonate, it cannot be determined if it was due to i) succinate buildup shifting succinate-CoA ligase equilibrium toward ATP (or GTP) utilization, ii) favoring itaconyl-CoA formation hydrolyzing ATP (or GTP) for the thioesterification, or iii) an ensuing CoA trap in the form of itaconyl-CoA, which could negatively affect the upstream supply of succinyl-CoA from the KGDHC (Kiss et al., 2013), in turn diminishing ATP (or GTP) formation through SLP by succinate-CoA ligase. In support of points ii) and iii), the succinate-CoA ligase inhibitor KM4549SC, which does not inhibit SDH exerted a similar effect as itaconate on $\Delta\Psi m$ of respiration-inhibited mitochondria. Regarding the impact of ATP (or GTP) hydrolysis caused by itaconyl-CoA formation *vice versa* the sequestration of CoA negatively affecting the upstream supply of succinyl-CoA from the KGDHC and in turn the reaction catalyzed by succinate-CoA ligase toward SLP, the latter concept is probably more important: the

catalytic efficiency of succinate-CoA ligase with itaconate is likely to be smaller than that for succinate; indeed, bacterial succinate-CoA ligases exhibit 2- to 10-fold higher K_m values for itaconate compared with those for succinate (Nolte et al., 2014). Furthermore, biosynthesis of 1 CoA molecule requires the expenditure of 4 ATP molecules (Theodoulou et al., 2014). Therefore, the itaconate-induced sequestration of CoA in the form of itaconyl-CoA (which metabolizes very slowly in mammalian cells) decreasing the upstream supply of succinyl-CoA from the KGDHC (Kiss et al., 2013), and in turn affecting the reaction catalyzed by succinate-CoA ligase toward formation of ATP (or GTP), results in a more pronounced effect diminishing SLP, than that of hydrolyzing ATP (or GTP) for the thioesterification of itaconate by succinate-CoA ligase.

The significance of our findings is, to mount an immune defense, cells of macrophage lineage may lose their capacity of mitochondrial SLP for producing itaconate. Having said that, the question arises as of what would be the consequences of mitochondrial SLP inhibition during infection *in vivo*? This is difficult to address, primarily because that would have been done through induction of *Acod1* through LPS (or an appropriate infection), a maneuver that inherently induces concomitant alterations in glycolysis and oxidative phosphorylation. Under these conditions, it would be challenging to decipher which bioenergetic (or any other) effects are attributed to glycolysis and/or oxidative phosphorylation and/or mitochondrial SLP. Limitations in oxygen availability (that could greatly upregulate glycolysis and diminish oxidative phosphorylation) where SLP by succinate-CoA ligase is afforded a much more prominent role regarding mitochondrial bioenergetics (Weinberg et al., 2000; Chinopoulos et al., 2010; Chinopoulos, 2011a,b; Kiss et al., 2013), could only occur in macrophages infiltrating oxygen-depleted tissues (*i.e.*, infections with hypoxic cores, or rapidly expanding solid tumors). In such environments, production of itaconate by infiltrating macrophages would have dual, but opposing roles: itaconate would decrease the survival of the infective microbes (or the tumor cells, should they rely on SLP for energy harnessing in view of a pertaining hypoxia), but on the other hand it would also decrease the ability of the macrophage producing it to cope under the same bioenergetic stress of hypoxia, as discussed elsewhere (Weinberg et al., 2000; Chinopoulos et al., 2010; Chinopoulos, 2011a,b; Kiss et al., 2013).

Regarding the potential consequences of mitochondrial SLP inhibition during infection, it is also worth mentioning those for the infective organism. Inhibition of SLP of the infective organism could be detrimental; indeed, apart from the antimicrobial properties of itaconate (due to its effect on the glyoxylate shunt), mitochondrial SLP mediated by succinate-CoA ligase is essential for growth of procyclic *Trypanosoma brucei* (Bochud-Allemann and Schneider, 2002; Kiss et al., 2013), and likely other microbes relying on this oxygen-independent pathway. Internalization of macrophage-produced itaconate by the microbe would inhibit its SLP and decrease its chances for survival, thus thwarting the infection.

The subject of itaconate and its effect on SLP was extended and further investigated by taking in the account one more parameter: SUCL, which is located in the mitochondrial matrix and is the key enzyme in SLP. SUCL places itself in the intersection of several metabolic pathways (for details see Kacso et al., 2016), and it is not surprising that its deficiency leads to serious pathology. It is known that SUCL shows tissues-specific expression. This heterodimer enzyme is composed of invariant Suclg1 α-subunit and a substrate-specific Sucla2 or Suclg2 β-subuint yielding ATP or GTP, respectively. *SUCLA2* is highly expressed in skeletal muscle, brain and heart, while *SUCLG2* is barely detected in brain and muscle, but strongly expressed in liver and kidney. Furthermore, in the human brain, *SUCLA2* is exclusively expressed in the neurons, whereas *SUCLG2* is only found in cells forming the microvasculature. To date, patients with *SUCLA2* and *SUCLG1* gene deficiency have been reported, while there is no evidence of *SUCLG2* gene deficient patients – this type of mutation may be incompatible with life. The argument that *SUCLA2* is critical for SLP and is influenced by itaconate is underlined through series of experiments. For the detailed investigation Sucla2 +/– and Suclg2 +/– mice were generated. Homozygous knockout mice for either gene are not viable (Kacso et al., 2016). Implementing mRNA quantification, SUCL subunit expression and enzymatic activities, it was concluded that deletion of one *Sucla2* allele is associated with a decrease in Suclg1 expression and a rebound increase in Suclg2 expression, *i.e.*, GTP-forming SUCL activity is increased. On contrary, similar rebound effect wasn't detected in Suclg2 +/– mice. Because of the lack of a rebound and effect on Sucla2 expression in Suclg2 +/– mice, and the fact that *SUCLG2* deficiency has never been reported in humans only Sucla2 +/– transgenic strains was

investigated in presence of itaconate. No differences in mitochondrial respiration or SLP during chemical (rotenone) or true anoxia were observed by comparing Sucla2 +/– and wild type mice. The lack of effect could be explained by the rebound increases in Suclg2 expression and associated increases in GTP-forming SUCL activity that in turn could maintain SLP. The argument that *SUCLA2* is critical for SLP is strengthen by the findings where a concomitant submaximal inhibition of SUCL by itaconate revealed that mitochondria obtained from Sucla2 +/– mice are less able to perform SLP than wild type littermates.

Our work based on itaconate affecting one of the steps in TCA cycle, *i.e.* SLP, boosted the interest toward further research on itaconate. Two papers (Lampropoulou et al., 2016; Cordes et al., 2016) came out that claim on the fact that itaconate inhibits succinate dehydrogenase and through this act links itself to metabolism of macrophages and their role in inflammation. These data once more supported the importance of itaconate in biochemical pathways. As it is usual with interplaying molecules to be of clinical interest it is the same with itaconate and succinate. Inflammation provides diverse effects in human diseases where the succinate-SDH axis and its interaction with itaconate could be potent drug target.

This thesis as well as the papers following it reflects on the possibility that itaconate, as a regulatory molecule to reprogram immune cell metabolism, is the link between innate immunity, metabolism, and disease pathogenesis.

7. CONCLUSIONS

Based on the results elaborated throughout this thesis the following postulations could be concluded.

Itaconate abolishes SLP due to:

1. a “CoA trap” in the form of itaconyl-CoA that negatively affects the upstream supply of succinyl-CoA from the α-ketoglutarate dehydrogenase complex;
2. depletion of ATP (or GTP), which are required for the thioesterification by succinate-CoA ligase;
3. inhibition of complex II leading to a buildup of succinate which shifts succinate-CoA ligase equilibrium toward ATP (or GTP) utilization.

Our results support the notion that *Acod1*-expressing cells of macrophage lineage lose the capacity of mitochondrial SLP for producing itaconate during mounting of an immune defense.

To the present knowledge, in the human body only macrophages express *Acod1*, and therefore can produce itaconic acid. The realization that the switching on of *Acod1* interferes with normal metabolism could be useful for different applications, *e.g.*:

- Internalization of macrophage-produced itaconate by the microbe would inhibit its SLP and decrease its chances for survival, thus thwarting the infection.
- The introduction of *Acod1* in tumor cells could prove to be an efficient strategy for depleting the tumor from energy, thus thwarting its ability to grow.

8. SUMMARY

Itaconic acid is an unsaturated dicarboxylic acid which manifests antimicrobial effects by inhibiting isocitrate lyase, a key enzyme of the glyoxylate shunt. Recently it has been shown that in the cells of macrophage lineage itaconic acid is present as a product of an enzyme encoded by the gene *cis*-aconitate decarboxylase 1 (*Acod1*) (previous name: immunoresponsive gene 1, *Irg1*), which was localized to the mitochondria. The citric acid cycle intermediate, *cis*-aconitate decarboxylation is catalyzed by Acod1 to yield itaconic acid. In mitochondria, itaconate can be converted by succinate-CoA ligase to itaconyl-CoA at the expense of ATP (or GTP). Under normal conditions succinate-CoA ligase catalyzes the reversible conversion of succinyl-CoA and ADP (or GDP) to coenzyme A, succinate and ATP (or GTP). This step is known as substrate-level phosphorylation (SLP).

The aim of this thesis was to investigate the effects of increased itaconate production on SLP. To elucidate our presumptions we performed different experiments on *in situ* and isolated mitochondria. Experimental conditions were established by lipopolysaccharide (LPS)-induced stimulation of *Acod1* in bone marrow-derived macrophages (BMDM) and RAW-264.7 cells. In rotenone-treated macrophage cells, stimulation by LPS led to impairment in SLP of *in situ* mitochondria, deduced from the reversal operation of the adenine nucleotide translocase (ANT). Silencing experiments directed against *Acod1* expression with siRNA − but not scrambled siRNA − in LPS-induced RAW-264.7 cells reversed impairment in SLP. LPS dose-dependently inhibited oxygen consumption rates and elevated glycolysis rates in BMDM but not RAW-264.7 cells, studied under various metabolic conditions. In isolated mitochondria treated with rotenone, itaconate dose-dependently reversed the operation of ANT, implying impairment in SLP, an effect that was partially mimicked by malonate. However, malonate yielded greater ADP-induced depolarizations than itaconate.

As a conclusion, itaconate abolishes SLP by favouring itaconyl-CoA formation at the expense of ATP (or GTP), and/or inhibiting complex II leading to a build-up of succinate which shifts succinate-CoA ligase equilibrium towards ATP (or GTP) utilization.

9. ÖSSZEFOGLALÁS

Az itakonát antibakteriális hatású telítetlen dikarbonsav − az izocitrát liázt, a glioxilát ciklus kulcsenzimét gátolja. Kísérleti eredmények bizonyítják, hogy a makrofág sejtekben az itakonát a mitokondriumban lokalizált *cisz*-akonitát dekarboxiláz 1 (*Acod1*) (korábbi nevén: immunoresponsive gén 1, *Irg1*) által kódolt enzim terméke. A citrátciklus köztes termékét, a *cisz*-akonitát dekarboxilációját az Acod1 katalizálja, mely reakcióban itakonát keletkezik. A mitokondriumban az itakonátot a szukcinil-CoA-szintetáz ATP (vagy GTP) felhasználásával itakonil-CoA-vá alakítja. Normál körülmények között a a szukcinil-CoA-szintetáz egy reverzibilis reakciót katalizál, melynek során a szukcinil-CoA és ADP (vagy GDP) átalakul CoA-vá, szukcináttá és ATP-vé (vagy GDP-vé). Ez az átalakulás szubsztrátszintű foszforilációként ismert.

A célunk az volt, hogy a megemelkedett itakonát koncentrációjának a hatását vizsgáljuk a szubsztrátszintű foszforilációra. Az előfeltevéseink alátámasztása érdekében különböző kísérleteket végeztünk *in situ* és izolált mitokondriumon. A csontvelői sejtekből differenciáltatott makrofágokban (BMDM) és RAW-264.7 sejtekben lipopoliszaharid (LPS)-indukálta *Acod1* stimulációt alkalmaztunk a megfelelő kísérleti feltételek érdekében. A rotenonnal kezelt makrofágokban a LPS indukció meghiúsította a szubsztrátszintű foszforilációt az *in situ* mitokondriumokban, melyre az adeninnukleotid-transzporter (ANT) fordított működéséből lehetett következtetni. A csendesítési kísérletekben, a RAW-264.7 sejtekben az LPS-indukálta szubsztrátszintű foszforiláció meghiúsulását az *Acod1* ellen irányuló siRNS kezelés kivédte, míg a scrambled siRNS (a nem specifikus targetált kontroll) nem. Az LPS, különböző metabolikus feltételek között, koncentrációfüggően gátolta az oxigén fogyasztást és megemelte a glikolízis szintjét a BMDM sejtekben, de a RAW-264.7 sejtekben nem. A rotenonnal kezelt izolált mitokondriumban az itakonát koncentrációfüggően megfordította az ANT működését, utalva a szubsztrátszintű foszforiláció hibás működésére; a hatást részben utánozta a malonát. Ugyanakkor a malonát jelentősebb mértékű ADP-indukálta depolarizációt idézett elő, mint az itakonát.

Summa summarum, az itakonát meghiúsítja a szubsztrátszintű foszforilációt előnyben részesítve az itakonil-CoA képződését ATP (vagy GTP) rovására, és/vagy gátolja a komplex-II-t, ami a szukcinát felhalmozódásához vezet és eltolja a szukcinil-CoA-szintetáz egyensúlyát az ATP (vagy GTP) felhasználása felé.

10. BIBLIOGRAPHY

Abramov AY, Duchen MR. (2005) The role of an astrocytic NADPH oxidase in the neurotoxicity of amyloid beta peptides. *Philos Trans R Soc Lond B Biol Sci* 360, 2309-2314

Abramov AY, Duchen MR. (2008) Mechanisms underlying the loss of mitochondrial membrane potential in glutamate excitotoxicity. *Biochim Biophys Acta* 1777, 953-964

Adler J, Wang SF, Lardy HA. (1957) The metabolism of itaconic acid by liver mitochondria. *J Biol Chem* 229, 865-879

Åkerman KE, Wikström MK. (1976) Safranine as a probe of the mitochondrial membrane potential. *FEBS Lett* 68, 191-197

Allavena P, Sica A, Garlanda C, Mantovani A. (2008) The yin-yang of tumor-associated macrophages in neoplastic progression and immune surveillance. *Immunol Rev* 222, 155-161

Basler T, Jeckstadt S, Valentin-Weigand P, Goethe R. (2006) Mycobacterium paratuberculosis, Mycobacterium smegmatis, and lipopolysaccharide induce different transcriptional and post-transcriptional regulation of the IRG1 gene in murine macrophages. *J Leukoc Biol* 79, 628-638

Baup S. (1836) Über eine neue pyrogen-citronensäure, und über benennung der pyrogen-säuren überhaupt. *Ann Pharm* 19, 29-38

Bentley R, Thiessen CP. (1957a) Biosynthesis of itaconic acid in *Aspergillus terreus*. I. Tracer studies with C14-labeled substrates. *J Biol Chem* 226, 673-687

Bentley R, Thiessen CP. (1957b) Biosynthesis of itaconic acid in *Aspergillus terreus*. III. The properties and reaction mechanism of *cis*-aconitic acid decarboxylase. *J Biol Chem* 226, 703-720

Berg IA, Filatova LV, Ivanovsky RN. (2002) Inhibition of acetate and propionate assimilation by itaconate *via* propionyl-CoA carboxylase in isocitrate lyase-negative purple bacterium Rhodospirillum rubrum. *FEMS Microbiol Lett* 216, 49-54

Bochud-Allemann N, Schneider A. (2002) Mitochondrial substrate level phosphorylation is essential for growth of procyclic Trypanosoma brucei. *J Biol Chem* 277, 32849-32854

Bonnarme P, Gillet B, Sepulchre AM, Role C, Beloeil JC, Ducrocq C. (1995) Itaconate biosynthesis in *Aspergillus terreus*. *J Bacteriol* 177, 3573-3578

Booth AN, Taylor J, Wilson RH, Deeds F. (1952) The inhibitory effects of itaconic acid in vitro and in vivo. *J Biol Chem* 195, 697-702

Boyer PD. (2002) A research journey with ATP synthase. *J Biol Chem* 277, 39045-39061

Calam CT, Oxford AE, Raistrick H. (1939) Studies in the biochemistry of micro-organisms: itaconic acid, a metabolic product of a strain of *Aspergillus terreus* Thom. *Biochem J* 33, 1488-1495

Chávez-Galán L, Olleros ML, Vesin D, Garcia I. (2015) Much More than M1 and M2 Macrophages, There are also $CD169^+$ and TCR^+ Macrophages. *Front Immunol* 6, 263

Chinopoulos C, Vajda S, Csanady L, Mandi M, Mathe K, Adam-Vizi V. (2009) A novel kinetic assay of mitochondrial ATP-ADP exchange rate mediated by the ANT. *Biophys J* 96, 2490-2504

Chinopoulos C, Gerencser AA, Mandi M, Mathe K, Torocsik B, Doczi J, Turiak L, Kiss G, Konrad C, Vajda S, Vereczki V, Oh RJ, Adam-Vizi V. (2010) Forward operation of adenine nucleotide translocase during FoF1-ATPase reversal: critical role of matrix substrate-level phosphorylation. *FASEB J* 24, 2405-2416

Chinopoulos C. (2011a) The "B space" of mitochondrial phosphorylation. *J Neurosci Res* 89, 1897-1904

Chinopoulos C. (2011b) Mitochondrial consumption of cytosolic ATP: not so fast. *FEBS Lett* 585, 1255-1259

Cho H, Proll SC, Szretter KJ, Katze MG, Gale M, Diamond MS. (2013) Differential innate immune response programs in neuronal subtypes determine susceptibility to infection in the brain by positivestranded RNA viruses. *Nat Med* 19, 458-64

Cordes T, Michelucci A, Hiller K. (2015) Itaconic acid: the surprising role of an industrial compound as a mammalian antimicrobial metabolite. *Annu Rev Nutr* 35, 451-473

Cordes T, Wallace M, Michelucci A, Divakaruni AS, Sapcariu SC, Sousa C, Koseki H, Cabrales P, Murphy AN, Hiller K, Metallo CM. (2016) Immunoresponsive gene 1

and itaconate inhibit succinate dehydrogenase to modulate intracellular succinate levels. *J Biol Chem* 291, 14274-14284

Degrandi D, Hoffmann R, Beuter-Gunia C, Pfeffer K. (2009) The proinflammatory cytokine-induced IRG1 protein associates with mitochondria. *J Interferon Cytokine Res* 29, 55-68

Dervartanian DV, Veeger C. (1964) Studies on succinate dehydrogenase. I. Spectral properties of the purified enzyme and formation of enzyme-competitive inhibitor complexes. *Biochim Biophys Acta* 92, 233-247

Dunn MF, Ramírez-Trujillo JA, Hernández-Lucas I. (2009) Major roles of isocitrate lyase and malate synthase in bacterial and fungal pathogenesis. *Microbiology* 155, 3166-3175

Ecker J, Liebisch G, Englmaier M, Grandl M, Robenek H, Schmitz G. (2010) Induction of fatty acid synthesis is a key requirement for phagocytic differentiation of human monocytes. *Proc Natl Acad Sci USA* 107, 7817-7822

El-Imam AA, Du C. (2014) Fermentative itaconic acid production. *J Biodivers Bioprospect Dev* 1, 1-8

Ernster L. (1958a) Diaphorase activities in liver cytoplasmic fractions. *Federation Proc* 17, 216

Ernster L, Navazio F. (1958b) Soluble diaphorase in animal tissues. *Acta Chem Scand* 12, 595-602

Everts B, Amiel E, van der Windt GJ, Freitas TC, Chott R, Yarasheski KE, Pearce E L, Pearce EJ (2012) Commitment to glycolysis sustains survival of NO-producing inflammatory dendritic cells. *Blood* 120, 1422-1431

Fang FC, Libby SJ, Castor ME, Fung AM. (2005) Isocitrate lyase (acea) is required for Salmonella persistence but not for acute lethal infection in mice. *Infect Immun* 73, 2547-2549

Feniouk BA, Yoshida M. (2008) Regulatory mechanisms of proton-translocating Fo-F1-ATP synthase. *Results Probl Cell Differ* 45, 279-308

Franke W, Holz E. (1957) Zur Kenntniss der Spezifität von Dehydrasen III Über Das Verhalten halogensubstituierter Bernsteinsäuren sowie einiger anderer Bernsteinsäure- und Malonsäure-Derivate gegenüber Succinodehydrase. *Justus Liebigs Ann Chem* 608, 168-194

Gerencser AA, Neilson A, Choi SW, Edman U, Yadava N, Oh RJ, Ferrick DA, Nicholls DG, Brand MD. (2009) Quantitative microplate-based respirometry with correction for oxygen. *Anal Chem* 81, 6868-6878

Gordon S, Taylor PR. (2005) Monocyte and macrophage heterogeneity. *Nat Rev Immunol* 5, 953-964

Gray MW, Burger G, Lang BF. (1999) Mitochondrial Evolution. *Science* 283, 1476-1481

Gyamerah MH. (1995) Oxygen requirement and energy relations of itaconic acid fermentation by *Aspergillus terreus* NRRL 1960. *Appl Microbiol Biotechnol* 44, 20-26

Haile DJ, Rouault TA, Harford JB, Kennedy MC, Blondin GA, Beinert H, Klausner RD. (1992) Cellular regulation of the iron-responsive element binding protein: disassembly of the cubane iron-sulfur cluster results in high-affinity RNA binding. *Proc Natl Acad Sci USA* 89, 11735-11739

Haskins RHR, Thorn JA, Boothroyd B. (1955) Biochemistry of the Ustilaginales. XI. Metabolic products of Ustilago zeae in submerged culture. *Can J Microbiol* 1, 749-756

Hilz H, Knappe J, Ringelmann E, Lynen F. (1958) [Methylglutaconase, a new hydrase participating in the metabolism of various carboxylic acids]. *Biochem Z* 329, 476-489

Hoebe K, Du X, Georgel P, Janssen E, Tabeta K, Kim SO, Goode J, Lin P, Mann N, Mudd S, Crozat K, Sovath S, Han J, Beutler B. (2003) Identification of Lps2 as a key transducer of MyD88-independent TIR signalling. *Nature* 424, 743-748

Hoentjen F, Sartor RB, Ozaki M, Jobin C. (2005) STAT3 regulates NF-kappaB recruitment to the IL-12p40 promoter in dendritic cells. *Blood* 105, 689-696

Hoshino K, Kaisho T, Iwabe T, Takeuchi O, Akira S. (2002) Differential involvement of IFN-β in toll-like receptor-stimulated dendritic cell activation. *Int Immunol* 14, 1225-1231

Hunger-Glaser I, Brun R, Linder M, Seebeck T. (1999) Inhibition of succinyl CoA synthetase histidine-phosphorylation in Trypanosoma brucei by an inhibitor of bacterial two-component systems. *Mol Biochem Parasitol* 100, 53-59

Jahngen JH, Rossomando EF. (1983) Resolution of an ATP-metal chelate from metal-free ATP by reverse-phase high-performance liquid chromatography. *Anal Biochem* 130, 406-415

Jaklitsch WM, Kubicek CP, Scrutton MC. (1991) The subcellular organization of itaconate biosynthesis in *Aspergillus terreus*. *J Gen Microbiol* 137, 533-539

Johnson JD, Mehus JG, Tews K, Milavetz BI, Lambeth DO. (1998a) Genetic evidence for the expression of ATP- and GTP-specific succinyl-CoA synthetases in multicellular eucaryotes. *J Biol Chem* 273, 27580-27586

Johnson JD, Muhonen WW, Lambeth DO. (1998b) Characterization of the ATP- and GTP-specific succinyl-CoA synthetases in pigeon. The enzymes incorporate the same alpha-subunit. *J Biol Chem* 273, 27573-27579

Kacso G, Ravasz D, Doczi J, Németh B, Madgar O, Saada A, Ilin P, Miller C, Ostergaard E, Iordanov I, Adams D, Vargedo Z, Araki M, Araki K, Nakahara M, Ito H, Gál A, Molnár MJ, Nagy Z, Patocs A, Adam-Vizi V, Chinopoulos C. (2016) Two transgenic mouse models for β-subunit components of succinate-CoA ligase yielding pleiotropic metabolic alterations. *Biochem J* 15, 3463-3485

Kawamura D, Furuhashi M, Saito O, Matsui H. (1981) Production of itaconic acid by fermentation. *Japan Patent* 56137893

Kelly B, O'Neill LA. (2015) Metabolic reprogramming in macrophages and dendritic cells in innate immunity. *Cell Res* 25, 771-784

Kimura A, Naka T, Nakahama T, Chinen I, Masuda K, Nohara K, Fujii-Kuriyama Y, Kishimoto T. (2009) Aryl hydrocarbon receptor in combination with Stat1 regulates LPS-induced inflammatory responses. *J Exp Med* 206, 2027-2035

Kinoshita K. (1931) Über eine neue Aspergillus-Art, Asp. itaconicus nov. spec. *Bot Mag Tokyo* 45, 45-50

Kiss G, Konrad C, Doczi J, Starkov AA, Kawamata H, Manfredi G, Zhang SF, Gibson GE, Beal MF, Adam-Vizi V, Chinopoulos C. (2013) The negative impact of α-ketoglutarate dehydrogenase complex deficiency on matrix substrate-level phosphorylation. *FASEB J* 27, 2392-2406

Kiss G, Konrad C, Pour-Ghaz I, Mansour JJ, Nemeth B, Starkov AA, Adam-Vizi V, Chinopoulos C. (2014) Mitochondrial diaphorases as NAD^+ donors to segments of

the citric acid cycle that support substrate-level phosphorylation yielding ATP during respiratory inhibition. *FASEB J* 28, 1682-1697

Kitamura T, Qian BZ, Pollard JW. (2015) Immune cell promotion of metastasis. *Nat Rev Immunol* 15, 73-86

Klement T, Milker S, Jäger G, Grande P M, Domínguez de María P, Büchs J. (2012) Biomass pretreatment affects Ustilago maydis in producing itaconic acid. *Microb Cell Fact* 11, 43

Klingenberg M. (2008) The ADP and ATP transport in mitochondria and its carrier. *Biochim Biophys Acta* 1778, 1978-2021

Komohara Y, Jinushi M, Takeya M. (2014) Clinical significance of macrophage heterogeneity in human malignant tumors. *Cancer Sci* 105, 1-8

Komohara Y, Fujiwara Y, Ohnishi K, Takeya M. (2016) Tumor-associated macrophages: Potential therapeutic targets for anti-cancer therapy. *Adv Drug Deliv Rev* 99, 180-185

Krawczyk CM, Holowka T, Sun J, Blagih J, Amiel E, DeBerardinis RJ, Cross JR, Jung E, Thompson CB, Jones RG, Pearce EJ. (2010) Toll-like receptor-induced changes in glycolytic metabolism regulate dendritic cell activation. *Blood* 115, 4742-4749

Kumar R. (2009) Glyoxylate shunt: combating mycobacterium at forefront. *Int J Integr Biol* 7, 69-72

Kvitvang HF, Andreassen T, Adam T, Villas-Bôas SG, Bruheim P. (2011) Highly sensitive GC/MS/MS method for quantitation of amino and nonamino organic acids. *Anal Chem* 83, 2705-2711

Labbe RF, Kurumada T, Onisawa J. (1965) The role of succinyl-CoA synthetase in the control of heme biosynthesis. *Biochim Biophys Acta* 111, 403-415

Lambeth DO, Tews KN, Adkins S, Frohlich D, Milavetz BI. (2004) Expression of two succinyl-CoA synthetases with different nucleotide specificities in mammalian tissues. *J Biol Chem* 279, 36621-36624

Lampropoulou V, Sergushichev A, Bambouskova M, Nair S, Vincent EE, Loginicheva E, Cervantes-Barragan L, Ma X, Huang SC, Griss T, Weinheimer CJ, Khader S, Randolph GJ, Pearce EJ, Jones RG, Diwan A, Diamond MS, Artyomov MN. (2016) Itaconate links inhibition of succinate dehydrogenase with macrophage metabolic remodeling and regulation of inflammation. *Cell Metab* 24, 158-166

Lee Y, Sohn WJ, Kim DS, Kwon HJ. (2004) NF-kappaB- and c-Jun-dependent regulation of human cytomegalovirus immediate-early gene enhancer/promoter in response to lipopolysaccharide and bacterial CpG-oligodeoxynucleotides in macrophage cell line RAW-264.7. *Eur J Biochem* 271, 1094-1105

Li H, Gang Z, Yuling H, Luokun X, Jie X, Hao L, Li W, Chunsong H, Junyan L, Mingshen J, Youxin J, Feili G, Boquan J, Jinquan T. (2006) Different neurotropic pathogens elicit neurotoxic CCR9- or neurosupportive CXCR3-expressing microglia. *J Immunol* 177, 3644-3656

Lin YH, Li YF, Huang MC, Tsai YC. (2004) Intracellular expression of vitreoscilla hemoglobin in *Aspergillus terreus* to alleviate the effect of a short break in aeration during culture. *Biotechnol Lett* 26, 1067-1072

Liu Y, Su WW, Wang S, Li PB. (2012) Naringin inhibits chemokine production in an LPS-induced RAW-264.7 macrophage cell line. *Mol Med Rep* 6, 1343-1350

Mantovani A, Biswas SK, Galdiero MR, Sica A, Locati M. (2013) Macrophage plasticity and polarization in tissue repair and remodelling. *J Pathol* 229, 176-185

McFadden BA, Williams JO, Roche TE. (1971) Mechanism of action of isocitrate lyase from *Pseudomonas indigofera*. *Biochemistry* 10, 1384-1390

McKinney JD, Höner zu Bentrup K, Muñoz-Elías EJ, Miczak A, Chen B, Chan WT, Swenson D, Sacchettini JC, Jacobs WR Jr, Russell DG. (2000) Persistence of Mycobacterium tuberculosis in macrophages and mice requires the glyoxylate shunt enzyme isocitrate lyase. *Nature* 406, 735-738

Ménage S, Attrée I. (2014) Pathogens love the poison. *Nat Chem Biol* 10, 326-327

Metelkin E, Demin O, Kovacs Z, Chinopoulos C. (2009) Modeling of ATP-ADP steady-state exchange rate mediated by the adenine nucleotide translocase in isolated mitochondria. *FEBS J* 276, 6942-6955

Michelucci A, Cordes T, Ghelfi J, Pailot A, Reiling N, Goldmann O, Binz T, Wegner A, Tallam A, Rausell A, Buttini M, Linster C L, Medina E, Balling R, Hiller K. (2013) Immune-responsive gene 1 protein links metabolism to immunity by catalyzing itaconic acid production. *Proc Natl Acad Sci USA* 110, 7820-7825

Mills CD, Kincaid K, Alt JM, Heilman MJ, Hill AM. (2000) M-1/M-2 macrophages and the Th1/Th2 paradigm. *J Immunol* 164, 6166-6173

Mills CD, Lenz LL, Harris RA. (2016) A breakthrough: macrophage-directed cancer immunotherapy. *Cancer Res* 76, 513-516

Mills E, O'Neill LA. (2014) Succinate: a metabolic signal in inflammation. *Trends Cell Biol* 24, 313-320

Mookerjee SA, Goncalves RL, Gerencser AA, Nicholls DG, Brand MD. (2015) The contributions of respiration and glycolysis to extracellular acid production. *Biochim Biophys Acta* 1847, 171-181

Muñoz-Elías EJ, McKinney JD. (2006) Carbon metabolism of intracellular bacteria. *Cell Microbiol* 8, 10-22

Nathan CF. (2008) Metchnikoff's legacy in 2008. *Nature Immunol* 9, 695-698

Nelson DL, Cox MM. Lehninger Principles of Biochemistry, W. H. Freeman and Company, New York, 2008

Nolte JC, Schürmann M, Schepers CL, Vogel E, Wübbeler JH, Steinbüchel, A. (2014) Novel characteristics of succinate coenzyme A (Succinate-CoA) ligases: conversion of malate to malyl-CoA and CoA-thioester formation of succinate analogues *in vitro*. *Appl Environ Microbiol* 80, 166-176

Okabe M, Lies D, Kanamasa S Park, EY. (2009) Biotechnological production of itaconic acid and its biosynthesis in *Aspergillus terreus*. *Appl Microbiol Biotechnol* 84, 597-606

Ottaway JH, McClellan JA, Saunderson CL. (1981) Succinic thiokinase and metabolic control. *Int J Biochem* 13, 401-410

Pandey AK, Sassetti CM. (2008) Mycobacterial persistence requires the utilization of host cholesterol. *PNAS* 1054, 376-380

Pearce EL, Pearce EJ. (2013) Metabolic pathways in immune cell activation and quiescence. *Immunity* 38, 633-643

Phillips D, Aponte AM, French SA, Chess DJ, Balaban RS. (2009) Succinyl-CoA synthetase is a phosphate target for the activation of mitochondrial metabolism. *Biochemistry* 48, 7140-7149

Preusse M, Tantawy MA, Klawonn F, Schughart K, Pessler F. (2013) Infection- and procedure-dependent effects on pulmonary gene expression in the early phase of influenza A virus infection in mice. *BMC Microbiol* 13, 293

Qian BZ, Pollard JW. (2010) Macrophage diversity enhances tumor progression and metastasis. *Cell* 141, 39-51

Rodríguez-Prados JC, Través PG, Cuenca J, Rico D, Aragonés J, Martín-Sanz P, Cascante M, Boscá L. (2010) Substrate fate in activated macrophages: a comparison between innate, classic, and alternative activation. *J Immunol* 185, 605-614

Rosin DL, Okusa MD. (2011) Dangers within: DAMP responses to damage and cell death in kidney disease. *J Am Soc Nephrol* 22, 416-425

Russell DG, VanderVen BC, Lee W, Abramovitch RB, Kim MJ, Homolka S, Niemann S, Rohde KH. (2010) Mycobacterium tuberculosis wears what it eats. *Cell Host Microbe* 8, 68-76

Saada A, Bar-Meir M, Belaiche C, Miller C, Elpeleg O. (2004) Evaluation of enzymatic assays and compounds affecting ATP production in mitochondrial respiratory chain complex I deficiency. *Anal Biochem* 335, 66-72

Sakai A, Kusumoto A, Kiso Y, Furuya E. (2004) Itaconate reduces visceral fat by inhibiting fructose 2,6-bisphosphate synthesis in rat liver. *Nutrition* 20, 997-1002

Sanadi DR, Gibson M, Yengar P. (1954) Guanosine triphosphate, the primary product of phosphorylation coupled to the breakdown of succinyl coenzyme A. *Biochim Biophys Acta* 14, 434-436

Sasikaran J, Ziemski M, Zadora PK, Fleig A, Berg IA. (2014) Bacterial itaconate degradation promotes pathogenicity. *Nat Chem Biol* 10, 371-377

Scott ID, Nicholls DG. (1980) Energy transduction in intact synaptosomes. Influence of plasma-membrane depolarization on the respiration and membrane potential of internal mitochondria determined in situ. *Biochem J* 186, 21-33

Senior AE, Nadanaciva S, Weber J. (2002) The molecular mechanism of ATP synthesis by F1Fo-ATP synthase. *Biochim Biophys Acta* 1553, 188-211

Sharma V, Sharma S, Hoener zu Bentrup K, McKinney JD, Russell DG, Jacobs WR Jr, Sacchettini JC. (2000) Structure of isocitrate lyase, Mycobacterium tuberculosis. *Nat Struct Biol* 7, 663-668

Shin JH, Yang JY, Jeon BY, Yoon YJ, Cho SN, Kang YH, Ryu H, Hwang GS. (2011) (1)H NMR-based metabolomic profiling in mice infected with Mycobacterium tuberculosis. *J Proteome Res* 10, 2238-2247

Smith J, Sadeyen JR, Paton IR, Hocking PM, Salmon N, Fife M, Nair V, Burt DW, Kaiser P. (2011) Systems analysis of immune responses in Marek's disease virus-infected chickens identifies a gene involved in susceptibility and highlights a possible novel pathogenicity mechanism. *J Virol* 85, 11146-11158

Smith PK, Krohn RI, Hermanson GT, Mallia AK, Gartner FH, Provenzano MD, Fujimoto EK, Goeke NM, Olson BJ, Klenk DC. (1985) Measurement of protein using bicinchoninic acid. *Anal Biochem* 150, 76-85

Steiger MG, Blumhoff M L, Mattanovich D, Sauer M. (2013) Biochemistry of microbial itaconic acid production. *Front Microbiol* 4, 23

Strelko CL, Lu W, Dufort FJ, Seyfried TN, Chiles TC, Rabinowitz JD, Roberts MF. (2011) Itaconic acid is a mammalian metabolite induced during macrophage activation. *J Am Chem Soc* 133, 16386-16389

Stryer L. Biochemistry, W.H. Freeman, New York, 1995

Sugimoto M, Sakagami H, Yokote Y, Onuma H, Kaneko M, Mori M, Sakaguchi Y, Soga T, Tomita M. (2012) Non-targeted metabolite profiling in activated macrophage secretion. *Metabolomics* 8, 624-633

Tabuchi T, Sigisawa T, Ishidori T, Nakahara T, Sugiyama J. (1981) Itaconic acid fermentation by a yeast belonging to the genus Candida. *Agric Biol Chem* 45, 475-479

Tannahill GM, Curtis AM, Adamik J, Palsson-McDermott EM, McGettrick AF, Goel G, Frezza C, Bernard NJ, Kelly B, Foley NH, Zheng L, Gardet A, Tong Z, Jany SS, Corr SC, Haneklaus M, Caffrey BE, Pierce K, Walmsley S, Beasley FC, Cummins E, Nizet V, Whyte M, Taylor CT, Lin H, Masters SL, Gottlieb E, Kelly VP, Clish C, Auron PE, Xavier RJ, O'Neill LA. (2013) Succinate is an inflammatory signal that induces IL-1beta through HIF-1alpha. *Nature* 496, 238-242

Tavakoli S, Zamora D, Ullevig S, Asmis R. (2013) Bioenergetic profiles diverge during macrophage polarization: implications for the interpretation of 18F-FDG PET imaging of atherosclerosis. *J Nucl Med* 54, 1661-1667

Terakawa J, Wakitani S, Sugiyama M, Inoue N, Ohmori Y, Kiso Y, Hosaka YZ, Hondo E. (2011) Embryo implantation is blocked by intraperitoneal injection with anti-LIF antibody in mice. *J Reprod Dev* 57, 700-707

Theodoulous FL, Sibon OC, Jackowski S, Gout I. (2014) Coenzyme A and its derivatives: renaissance of a textbook classic. *Biochem Soc Trans* 42, 1025-1032

Thomas DM, Francescutti-Verbeem DM, Kuhn DM. (2006) Gene expression profile of activated microglia under conditions associated with dopamine neuronal damage. *FASEB J* 20, 515-517

Través PG, de Atauri P, Marín S, Pimentel-Santillana M, Rodríguez-Prados JC, Marín de Mas I, Selivanov VA, Martín-Sanz P, Boscá L, Cascante M. (2012) Relevance of the MEK/ERK signaling pathway in the metabolism of activated macrophages: a metabolomic approach. *J Immunol* 188, 1402-1410

Turner E. (1840) Elements of chemistry: including the recent discoveries and doctrines of the science. Philadelphia: Cowperthwait & Co.

Tyler DD, Gonze J. (1967) The preparation of heart mitochondria from laboratory animals. *Methods Enzymol* 10, 75-77

Upton AM, McKinney JD. (2007) Role of the methylcitrate cycle in propionate metabolism and detoxification in Mycobacterium smegmatis. *Microbiology* 153, 3973-3982

van der Geize R, Yam K, Heuser T, Wilbrink MH, Hara H, Anderton MC, Sim E, Dijkhuizen L, Davies JE, Mohn WW, Eltis LD. (2007) A gene cluster encoding cholesterol catabolism in a soil actinomycete provides insight into Mycobacterium tuberculosis survival in macrophages. *Proc Natl Acad Sci USA* 104, 1947-1952

van der Straat L, Vernooij M, Lammers M, van den Berg W, Schonewille T, Cordewener J, van der Meer I, Koops A, de Graaff LH. (2014) Expression of the *Aspergillus terreus* itaconic acid biosynthesis cluster in Aspergillus niger. *Microb Cell Fact* 13, 11

Vander Heiden MG, Cantley LC, Thompson CB. (2009) Understanding the Warburg effect: the metabolic requirements of cell proliferation. *Science* 324, 1029-1033

Vats D, Mukundan L, Odegaard JI, Zhang L, Smith KL, Morel CR, Wagner RA, Greaves DR, Murray PJ, Chawla A. (2006) Oxidative metabolism and PGC-1b attenuate macrophagemediated inflammation. *Cell Metab* 4, 13-24

Wang SF, Adler J, Lardy HA. (1961) The pathway of itaconate metabolism by liver mitochondria. *J Biol Chem* 236, 26-30

Warburg O. (1923) Metabolism of tumours. *Biochem Z* 142, 317-333

Weinberg JM, Venkatachalam MA, Roeser NF, Nissim I. (2000) Mitochondrial dysfunction during hypoxia/reoxygenation and its correction by anaerobic metabolism of citric acid cycle intermediates. *Proc Natl Acad Sci USA* 97, 2826-2831

West AP, Brodsky IE, Rahner C, Woo DK, Erdjument-Bromage H, Tempst P, Walsh MC, Choi Y, Shadel GS, Ghosh S. (2011) TLR signalling augments macrophage bactericidal activity through mitochondrial ROS. *Nature* 28, 476-480

Wibom C, Surowiec I, Mörén L, Bergström P, Johansson M, Antti H, Bergenheim AT. (2010) Metabolomic patterns in glioblastoma and changes during radiotherapy: a clinical microdialysis study. *J Proteome Res* 9, 2909-2919

Willke T, Vorlop KD. (2001) Biotechnological production of itaconic acid. *Appl Microbiol Biotechnol* 56, 289-295

Wu F, Yang F, Vinnakota KC, Beard DA. (2007) Computer modeling of mitochondrial tricarboxylic acid cycle, oxidative phosphorylation, metabolite transport, and electrophysiology. *J Biol Chem* 282, 24525-24537

Xaus J, Comalada M, Valledor AF, Lloberas J, Lopez-Soriano F, Argiles JM, Bogdan C, Celada A. (2000) LPS induces apoptosis in macrophages mostly through the autocrine production of TNF-alpha. *Blood* 95, 3823-3831

Xiao W, Wang L, Xiao R, Wu M, Tan J, He Y. (2011) Expression profile of human immune-responsive gene 1 and generation and characterization of polyclonal antiserum. *Mol Cell Biochem* 353, 177-187

Xu L, Shen S, Ma Y, Kim JK, Rodriguez-Agudo D, Heuman DM, Hylemon PB, Pandak WM, Ren S. (2012) 25-Hydroxycholesterol-3-sulfate attenuates inflammatory response *via* PPARgamma signaling in human THP-1 macrophages. *Am J Physiol Endocrinol Metab* 302, E788-E799

Yaffe MP. (1999) The Machinery of Mitochodrial Inheritance and Behavior. *Science* 283, 1493-1497

Yahiro K, Takahama T, Park YS, Okabe M. (1995) Breeding of *Aspergillus terreus* mutant TN-484 for itaconic acid production with high yield. *J Ferment Bioeng* 79, 506-508

Youle RJ, van der Bliek AM. (2012) Mitochondrial Fission, Fusion, and Stress. *Science* 337, 1062

Yu C, Cao Y, Zou H, Xian M. (2011) Metabolic engineering of Escherichia coli for biotechnological production of high-value organic acids and alcohols. *Appl Microbiol Biotechnol* 89, 573-583

Zhu L, Zhao Q, Yang T, Ding W, Zhao Y. (2015) Cellular metabolism and macrophage functional polarization. *Int Rev Immunol* 34, 82-100

11. BIBLIOGRAPHY OF THE CANDIDATE'S PUBLICATIONS

11.1. The publications related to the PhD thesis

Kiss G, Konrad C, Pour-Ghaz I, Mansour JJ, **Németh B**, Starkov AA, Adam-Vizi V, Chinopoulos C. (2014) Mitochondrial diaphorases as NAD^+ donors to segments of the citric acid cycle that support substrate-level phosphorylation yielding ATP during respiratory inhibition. *FASEB J* 28, 1682-1697 IF: 5.043

Németh B, Doczi J, Csete D, Kacso G, Ravasz D, Adams D, Kiss G, Nagy AM, Horvath G, Tretter L, Mócsai A, Csépányi-Kömi R, Iordanov I, Adam-Vizi V, Chinopoulos C. (2016) Abolition of mitochondrial substrate-level phosphorylation by itaconic acid produced by LPS-induced Irg1 expression in cells of murine macrophage lineage. *FASEB J* 30, 286-300 IF: 5.299

Kacso, G, Ravasz D, Doczi J, **Németh B**, Madgar O, Saada A, Ilin P, Miller C, Ostergaard E, Iordanov I, Adams D, Vargedo Z, Araki M, Araki K, Nakahara M, Ito H, Gál A, Molnár MJ, Nagy Z, Patocs A, Adam-Vizi V, Chinopoulos C. (2016) Two transgenic mouse models for β-subunit components of succinate-CoA ligase yielding pleiotropic metabolic alterations. *Biochem J* 15, 3463-3485 IF: 3.562

11.2. The publications not related to the PhD thesis

Hájos N, Pálhalmi J, Mann EO, **Németh B**, Paulsen O, Freund TF. (2004) Spike timing of distinct types of GABAergic interneuron during hippocampal gamma oscillations *in vitro*. *J Neurosci* 24, 9127-9137 IF: 7.907

Makara JK, Katona I, Nyiri G, **Nemeth B**, Ledent C, Watanabe M, de Vente J, Freund TF, Hajos N. (2007) Involvement of nitric oxide in depolarization-induced suppression of inhibition in hippocampal pyramidal cells during activation of cholinergic receptors. *J Neurosci* 27, 10211-10222 IF: 7.490

Haller J, Mátyás F, Soproni K, Varga B, Barsy B, **Németh B**, Mikics É, Freund TF, Hájos N. (2007) Correlated species differences in the effects of cannabinoid ligands on anxiety and on GABAergic and glutamatergic synaptic transmission. *Eur J Neurosci* 25, 2445-2456 IF: 3.673

Nemeth B, Ledent C, Freund TF, Hajos N. (2008) CB1 receptor-dependent and -independent inhibition of excitatory postsynaptic currents in the hippocampus by win 55,212-2. *Neuropharmacology* 54, 51-57 IF: 3.383

Holderith N, **Nemeth B**, Papp OI, Veres JM, Nagy GA, Hajos N. (2011) Cannabinoids attenuate hippocampal gamma oscillations by suppressing excitatory synaptic input onto CA3 pyramidal neurons and fast spiking basket cells. *J Physiol* 589, 4921-4934 IF: 4.881

Cserep C, Szonyi A, Veres JM, **Nemeth B**, Szabadits E, de Vente J, Hajos N, Freund TF, Nyiri G. (2011) Nitric oxide signaling modulates synaptic transmission during early postnatal development. *Cereb Cortex* 21, 2065-2074 IF: 6.544

Peterfi Z, Urban GM, Papp OI, **Nemeth B**, Monyer H, Szabo G, Erdelyi F, Mackie K, Freund TF, Hajos N, Katona I. (2012) Endocannabinoid-mediated long-term depression of afferent excitatory synapses in hippocampal pyramidal cells and GABAergic interneurons. *J Neurosci* 32, 14448-14463 IF: 6.908

Hajos N, Holderith N, **Nemeth B**, Papp OI, Szabo GG, Zemankovics R, Freund TF, Haller J. (2012) The effects of an echinacea preparation on synaptic transmission and the firing properties of CA1 pyramidal cells in the hippocampus. *Phytother Res* 26, 354-362 IF: 2.068

Hajos N, Karlocai MR, **Nemeth B**, Ulbert I, Monyer H, Szabo G, Erdelyi F, Freund TF, Gulyas AI. (2013) Input-output features of anatomically identified CA3 neurons during hippocampal sharp wave/ripple oscillation *in vitro*. *J Neurosci* 33, 11677-11691 IF: 6.747

12. ACKNOWLEDGEMENTS

I am most grateful to my supervisor, **Christos Chinopoulos, Ph.D**, for guiding my work and giving constructive pieces of advice. He is also to be thanked for the Western blot and immunocytochemistry experiments. I also would like to thank **Prof. Veronika Ádám-Vizi** and **Prof. László Tretter** for providing opportunity to work at the Department of Medical Biochemistry at Semmelweis University.

I am thankful to all the scientists who contributed to the research that provided the basis of this thesis: **Dániel Csete, Ph.D** for BMDMs, TIPMs and RAW-264.7 cells preparation; **Judit Dóczi, Ph.D** for imaging; **Iordan Iordanov, Ph.D** for providing FLAG protein; **Ádám Nagy, Pharm.D** and **Gergő Horváth, MD** for Seahorse measurements; **Roland Csépányi-Kömi, Ph.D** for siRNA; **Dóra Ravasz, Pharm.D** and **Gergely Kacsó, Pharm.D** for everyday experiments and data analysis, as well as discussions.

I am grateful to **Zsófia Nemoda, Ph.D** for demonstrating exceptional patience, kindness and scientific knowledge while supporting me to find just the right shaping for the thesis. Her insightful feedback helped me clean up my thoughts.

Furthermore I would like to express my gratitude toward those people at the department who were always kind to me, whose presence made a day brighter and times of doubt bearable.

At last, but not at least, I am honestly thankful to my family and friends on their support.